

Cobble: Compiling Block Encodings for Quantum Computational Linear Algebra

CHARLES YUAN, University of Wisconsin–Madison, USA

Quantum algorithms for computational linear algebra promise up to exponential speedups for applications such as simulation and regression, making them prime candidates for hardware realization. But these algorithms execute in a model that cannot efficiently store matrices in memory like a classical algorithm does, instead requiring developers to implement complex expressions for matrix arithmetic in terms of correct and efficient quantum circuits. Among the challenges for the developer is navigating a cost model in which conventional optimizations for linear algebra, such as subexpression reuse, can be inapplicable or unprofitable.

In this work, we present Cobble, a language for programming with quantum computational linear algebra. Cobble enables developers to express and manipulate the quantum representations of matrices, known as block encodings, using high-level notation that automatically compiles to correct quantum circuits. Cobble features analyses that compute the time and space usage of programs, as well as optimizations that reduce overhead and generate efficient circuits using state-of-the-art techniques such as the quantum singular value transformation. We evaluate Cobble on benchmark kernels for simulation, regression, search, and other applications, showing $2.6\times$ – $25.4\times$ speedups on these benchmarks compared to the unoptimized baseline.

CCS Concepts: • **Computer systems organization** → **Quantum computing**.

Additional Key Words and Phrases: quantum programming languages, quantum compilers

ACM Reference Format:

Charles Yuan. 2026. Cobble: Compiling Block Encodings for Quantum Computational Linear Algebra. *Proc. ACM Program. Lang.* 10, PLDI, Article 177 (June 2026), 26 pages. <https://doi.org/10.1145/3808255>

1 INTRODUCTION

Linear algebra is among the most promising applications of a quantum computer. A quantum state of n qubits encodes a vector of 2^n elements, enabling quantum algorithms to solve certain problems in linear systems [Harrow et al. 2009], physical simulation [Childs and Wiebe 2012], regression [Chakraborty et al. 2023], and differential equations [Berry 2014] in time polylogarithmic in the problem dimension. In suitable settings, the speedup over classical methods is exponential.

Practically realizing these speedups, however, poses a programming challenge even as hardware continues to advance [Bluvstein et al. 2023; Google Quantum AI 2025] toward the eventual availability of a scalable, fault-tolerant quantum computer. A quantum algorithm cannot efficiently store arbitrary matrices in memory like a classical algorithm does, because just processing every element would itself take linear time, limiting the possible speedup. Instead, quantum algorithms manipulate implicit representations of matrices that exploit structure, such as sparsity and factorization, using a tool called *block encoding* [Gilyén et al. 2019; Low and Chuang 2019; Martyn et al. 2021].

Author’s Contact Information: Charles Yuan, University of Wisconsin–Madison, USA, charlesyuan@cs.wisc.edu.



This work is licensed under a [Creative Commons Attribution 4.0 International License](https://creativecommons.org/licenses/by/4.0/).

© 2026 Copyright held by the owner/author(s).

ACM 2475-1421/2026/6-ART177

<https://doi.org/10.1145/3808255>

Block Encoding. Every quantum state is a unit vector, and every circuit of quantum logic gates is a unitary matrix. A *block encoding* of a matrix A is a unitary matrix with A embedded in its top left block. This concept enables a quantum circuit to implement a non-unitary A as a part of a larger unitary computation, to multiply A with a vector by applying the circuit to a quantum state, and to perform arithmetic on matrices given that $A + B$ may not be unitary even if A and B are.

A research paper specifies a quantum algorithm f on an input A by giving matrix arithmetic to turn a block encoding of A into $f(A)$. In a linear solver, $f(A) = A^{-1}$; in simulation [Gilyén et al. 2019], $f(A) = e^{-iAt}$; and in search [Martyn et al. 2021], $f(A) = \text{sign}(A) = A(A^2)^{-1/2}$. A paper typically explains how $f(A)$ can be built from arithmetic operators, e.g. $A^{-1} = I + (I - A) + (I - A)^2 + \dots$. Many papers [Camps et al. 2024; Sünderhauf et al. 2024] also show how a block encoding of the desired input A can be built from sums $B + C$, products $B \cdot C$, and tensor products $B \otimes C$ of realizable parts such as primitive logic gates or black-box circuits given as oracles.

Abstraction Challenge. To translate the block encoding arithmetic in an algorithms paper into a program to run on hardware, a developer could search for circuit constructions for matrix operators such as addition. A hurdle is that existing quantum programming languages such as Silq [Bichsel et al. 2020], Q# [Svore et al. 2018], and Qiskit [Javadi-Abhari et al. 2024] do not provide abstractions for creating and manipulating block encodings. They instead enable the developer to explicitly specify bit-level logic gates for each matrix expression, which for many linear algebra applications would be millions of gates [Scherer et al. 2017]. Block encodings present an opportunity to design new abstractions that ease this burden for developers of libraries and applications.

Efficiency Challenge. Reasoning about block encodings is essential not only to specify but also to optimize quantum algorithms, where they often act as performance bottlenecks [Li et al. 2023; Nibbi and Mendl 2024]. This reasoning is hard due to an unconventional cost model. The cost of a block encoding is given by not just its number of logic gates, but also a multiplier called *subnormalization* that dictates how many repetitions of the program are needed to produce the correct answer. This factor is not obvious from the literal length of a program and must be calculated separately.

Moreover, different ways to build the same matrix may be cheaper or costlier. A simple example is A vs. $\frac{1}{2}(A + A)$, which uses twice as many gates. A more subtle concern is that classical techniques to optimize linear algebra, such as subexpression reuse, can be unprofitable in quantum programs. For example, there is no general mechanism to compute a block encoding of $(A + B) \cdot (A + B)$ via just one addition and one multiplication by reusing the intermediate value of $A + B$.

Programming with Block Encodings. To bridge the abstraction gap, we present Cobble, a language to build and compose block encodings. Cobble offers high-level mathematical operators for matrix arithmetic, including sum, product, tensor product, and choice. In Cobble, a developer specifies block encodings for basic matrices using standard gates or application-specific circuits, and then composes them together using these mathematical operators. Like the Eigen [Guennebaud et al. 2010] linear algebra library but unlike prior quantum circuit languages, Cobble enables a developer to implement an algorithm using publication-style math notation rather than logic gates alone.

The Cobble compiler automatically translates a high-level program to a circuit to run on hardware, while the Cobble type system guarantees that every well-typed program has a valid circuit. Cobble also provides a cost model, derived from theory research, that a developer can use to compute the dominant factors in the time and space usage of programs, including subnormalization.

Optimizations for Block Encodings. To tackle the efficiency challenge, we present two optimizations for Cobble programs that reduce gate and subnormalization costs. The first, *sum fusion*, flattens nested linear combinations of matrices to remove intermediate overhead from subnormalization. The second, *polynomial fusion*, combines repeated sums and products into a compact form that

has an efficient circuit given by the quantum singular value transformation [Gilyén et al. 2019]. These optimizations exploit the algebraic structure of block encodings, and are complementary to techniques for end-to-end circuit synthesis from arbitrary matrices [Hantzko et al. 2024].

We implement Cobble as an embedded language in Python. To establish benchmarks for the emerging domain of quantum linear algebra, we use Cobble to express a set of kernels for simulation, regression, and other applications. Our optimizations reduce their total runtime cost – gate count times subnormalization – by $2.6\times$ – $25.4\times$ over the unoptimized program. Cobble takes little compile time and can yield more speedup than existing circuit optimizers on these programs.

Contributions. In this work, we present the following contributions:

- Sec. 4: Cobble, a quantum programming language of mathematical operators over block-encoded matrices, in which well-typed programs compile to valid quantum circuits;
- Sec. 5: A cost model to calculate the time and space usage of Cobble programs, indicating when classical optimizations are inapplicable or unprofitable in the quantum setting;
- Sec. 6: The sum and polynomial fusion optimizations for Cobble, which underpin an optimizing rewrite system that is sound, cost-nonincreasing, and strongly normalizing; and
- Sec. 7: An evaluation on benchmarks for simulation, regression, and other applications that shows $2.6\times$ – $25.4\times$ reductions in total runtime cost over the unoptimized baseline.

Impact. Our work enables developers to express core components for quantum linear algebra using high-level notation rather than qubit-level circuits and to soundly reduce their runtime costs. These ideas pave way to more accurate estimates of hardware requirements, more useful and robust benchmarks and compilers, and more near-term demonstrations of quantum advantage.

2 BACKGROUND

This section briefly reviews mathematical concepts needed for this work. A reader familiar with quantum computation but not with quantum algorithms for linear algebra is encouraged to read Section 2.2. For more detail, see the texts of Lin [2022] and Nielsen and Chuang [2010].

2.1 Quantum Computation

A *qubit* exists in a *superposition* or linear combination $\lambda_0 |\theta\rangle + \lambda_1 |1\rangle$ of two vectors $|\theta\rangle = [1, 0]^\top$ and $|1\rangle = [0, 1]^\top$, where $\lambda_0, \lambda_1 \in \mathbb{C}$ are *amplitudes* satisfying $|\lambda_0|^2 + |\lambda_1|^2 = 1$. Examples of qubits include $|\theta\rangle$, $|1\rangle$, and the states $\frac{1}{\sqrt{2}}(|\theta\rangle + e^{i\varphi} |1\rangle)$ where $\varphi \in [0, 2\pi)$ is known as a *phase*.

A *quantum state* of n qubits is a superposition over n -bit strings. For example, $\frac{1}{\sqrt{2}}(|\theta\theta\rangle + |11\rangle)$ is a quantum state over two qubits. Formally, multiple component states combine via the *tensor product* \otimes of vectors, such that the state $|\theta 1\rangle$ is defined as $|\theta\rangle \otimes |1\rangle$. We use the customary notations $|\theta 1\rangle$, $|\theta, 1\rangle$, and $|\theta\rangle |1\rangle$ to denote $|\theta\rangle \otimes |1\rangle$, and the notation $|\theta\rangle^{\otimes n}$ to denote n copies of $|\theta\rangle$.

Unitary Operators. A *quantum logic gate* manipulates the bit strings and their amplitudes within a quantum state without collapsing the state from superposition. The semantics of a quantum gate is a unitary matrix U – a linear, norm-preserving, and invertible operator with $U^{-1} = U^\dagger$.

The quantum gates over a single qubit include the NOT gate $X = \begin{bmatrix} 0 & 1 \\ 1 & 0 \end{bmatrix}$, mapping $|x\rangle \mapsto |1-x\rangle$ for $x \in \{0, 1\}$; the phase flip gate $Z = \begin{bmatrix} 1 & 0 \\ 0 & -1 \end{bmatrix}$, mapping $|x\rangle \mapsto (-1)^x |x\rangle$; the $\pi/4$ rotation gate T , mapping $|x\rangle \mapsto e^{ix\pi/4} |x\rangle$; and the Hadamard gate H , mapping $|x\rangle \mapsto \frac{1}{\sqrt{2}}(|\theta\rangle + (-1)^x |1\rangle)$.

The effect of a gate may be *controlled* by one or more qubits. For example, the two-qubit CNOT gate maps $|\theta, x\rangle \mapsto |\theta, x\rangle$ and $|1, x\rangle \mapsto |1, \text{NOT } x\rangle = |1, 1-x\rangle$. The three-qubit Toffoli gate is the quantum analogue of AND, mapping $|1, 1, x\rangle \mapsto |1, 1, 1-x\rangle$ only if the first two qubits are 1.

Measurement. A *measurement* probabilistically collapses the superposition of a quantum state into a classical outcome. When a qubit $\lambda_0 |\theta\rangle + \lambda_1 |1\rangle$ is measured in the standard basis, the observed classical outcome is θ with probability $|\lambda_0|^2$ and 1 with probability $|\lambda_1|^2$.

A composite state is *entangled* when it cannot be written as a tensor product of its components. The *Bell state* $\frac{1}{\sqrt{2}}(|\theta\theta\rangle + |11\rangle)$ is entangled, since it cannot be written as a product of two separate qubits. Given an entangled state, measuring one of its components causes the superposition of the other component to also collapse. For example, measuring the second qubit in the Bell state causes the first to also collapse, to either $|\theta\rangle$ or $|1\rangle$ with probability $|\frac{1}{\sqrt{2}}|^2 = \frac{1}{2}$ each.

2.2 Quantum Computational Linear Algebra

The essence of quantum algorithms for linear algebra is the ability of a quantum state or unitary operator to encode an exponentially large vector or matrix respectively:

Definition 2.1. Given a vector $x \in \mathbb{R}^N$ with $n = \log N$, its *amplitude encoding* is the n -qubit state

$$|x\rangle = \frac{1}{\|x\|_2} \sum_{j=0}^{N-1} x_j |j\rangle.$$

For example, two numbers can be encoded into the amplitudes of one qubit via the $R_y(\theta)$ gate, which takes $|\theta\rangle \mapsto \cos(\theta/2) |\theta\rangle + \sin(\theta/2) |1\rangle$. Efficient circuits to precisely encode vectors with higher dimension are an active area of research. General techniques applicable to our work include rotation trees with lookup tables [Low et al. 2024] and alias sampling [Babbush et al. 2018].

Definition 2.2. Given a matrix $A \in \mathbb{R}^{N \times N}$, a *block encoding* of A is any $(m+n)$ -qubit unitary

$$\mathcal{B}[A] = \begin{bmatrix} A/\alpha & \cdot \\ \cdot & \cdot \end{bmatrix},$$

where the top left block of the matrix is A rescaled by a *subnormalization* α satisfying $\alpha \geq \|A\|_2$, the spectral norm of A . The remaining blocks can be arbitrary as long as $\mathcal{B}[A]$ is unitary. Intuitively, we embed a possibly non-unitary A into any unitary $\mathcal{B}[A]$ representable by a quantum circuit.

Example 2.3. A unitary matrix U has itself as a block encoding $\mathcal{B}[U] = U$, using $m = 0$ additional qubits and $\alpha = 1$. In general, non-unitary matrices require $m \geq 1$ qubits to encode. For example,

$$\mathcal{B}[A] = \begin{bmatrix} A & \sqrt{I - A^2} \\ \sqrt{I - A^2} & -A \end{bmatrix}$$

is unitary for Hermitian A with $\|A\|_2 \leq 1$, using $m = 1$ qubit. More qubits are needed in practice.

A unitary operator that block-encodes a matrix A acts on a state that amplitude-encodes a vector x by matrix-vector multiplication Ax . Applying $\mathcal{B}[A]$ to $|x\rangle$ alongside m copies of $|\theta\rangle$ yields

$$\mathcal{B}[A] (|\theta\rangle^{\otimes m} |x\rangle) = \frac{\|Ax\|_2}{\alpha} |\theta\rangle^{\otimes m} |Ax\rangle + |\perp\rangle, \quad (2.1)$$

where $|Ax\rangle$ is a normalized amplitude encoding of Ax not scaled by α . An algorithm such as that of Harrow et al. [2009] can read out from this vector desired information such as its inner products.

Subnormalization. The state $|\perp\rangle$ is an undesirable failure case. Extracting $|Ax\rangle$ from the superposition requires *post-selection*: measuring the m temporary qubits, accepting if all yield $|\theta\rangle$, and starting over otherwise. Using amplitude amplification techniques [Berry et al. 2014], the expected number of rounds until success is $O(\alpha)$. Running time is thus proportional to subnormalization.

Matrix Arithmetic. Given $\mathcal{B}[A]$ and $\mathcal{B}[B]$, circuits are known that construct $\mathcal{B}[A + B]$, $\mathcal{B}[A \cdot B]$, $\mathcal{B}[A \otimes B]$, and other arithmetic operators [Gilyén et al. 2019]. For exposition, we describe next the construction of Childs and Wiebe [2012] to block-encode linear combinations of matrices.

Definition 2.4. Given $(m + n)$ -qubit operators that block-encode $A_j \in \mathbb{R}^{N \times N}$ and the coefficients $\lambda \in \mathbb{R}^L$ where $\ell = \log L$, a block encoding of $\sum_{j=0}^{L-1} \lambda_j A_j$ is the $(\ell + m + n)$ -qubit operator

$$\mathcal{B} \left[\sum_{j=0}^{L-1} \lambda_j A_j \right] = (\text{PREPARE}^\dagger \otimes I^{\otimes(m+n)}) \cdot \text{SELECT} \cdot (\text{PREPARE} \otimes I^{\otimes(m+n)}), \quad (2.2)$$

$$\text{where } \text{PREPARE}(|\theta\rangle^{\otimes \ell}) = \frac{1}{\sqrt{\|\lambda\|_1}} \sum_{j=0}^{L-1} \sqrt{|\lambda_j|} |j\rangle, \text{ and} \quad (2.3)$$

$$\text{SELECT}(|j\rangle |\theta\rangle^{\otimes m} |x\rangle) = \text{sign}(\lambda_j) |j\rangle \mathcal{B}[A_j] (|\theta\rangle^{\otimes m} |x\rangle). \quad (2.4)$$

Reading Equation 2.2 from right to left, the PREPARE operator first creates an amplitude encoding (Definition 2.1) into $|j\rangle$ of the coefficients $[\sqrt{\lambda_0}, \dots, \sqrt{\lambda_{L-1}}]$. Next, the SELECT operator chooses one of the $\mathcal{B}[A_j]$ to execute by controlling on the bits of $|j\rangle$. Finally, the inverse of the PREPARE operator restores $|j\rangle$ to zero to enable post-selection. The reason for taking square roots of the coefficients is that PREPARE and PREPARE[†] each incur a $\sqrt{|\lambda_j|}$ factor, which multiply to give the desired λ_j . Negative coefficients λ_j are handled by inserting a Z phase flip gate on each corresponding branch.

This method is known as *linear combination of unitaries* (LCU), so named for its original use case. It incurs a subnormalization that scales total runtime by $\alpha = \|\lambda\|_1 = \sum_j |\lambda_j|$. Negative λ_j increase α because the denominator of Equation 2.3 sums positive squared norms of amplitudes $\sqrt{|\lambda_j|}$.

Quantum Singular Value Transformation. A more general and efficient way to compute polynomials of block-encoded matrices is the *quantum singular value transformation* (QSVT) of Gilyén et al. [2019]. Given a block encoding of a Hermitian matrix A and a degree- d real polynomial $P(x)$ with fixed (even or odd) parity satisfying $|P(x)| \leq 1$ for all $x \in [-1, 1]$, QSVT computes the polynomial $P(A)$ via a circuit that applies a sequence of rotation gates interleaved with instances of $\mathcal{B}[A]$:

$$\mathcal{B}[P(A)] = e^{i\phi_0 Z_\Pi} \mathcal{B}[A] e^{i\phi_1 Z_\Pi} \dots e^{i\phi_{d-1} Z_\Pi} \mathcal{B}[A] e^{i\phi_d Z_\Pi}, \quad (2.5)$$

in which the Z_Π limits each phase rotation to the subspace $|\theta\rangle^{\otimes m}$ where all temporary qubits are zero. The phase angles ϕ_j are computed from the coefficients of $P(x)$ via a framework known as *quantum signal processing* (QSP) developed by Low and Chuang [2019]; Martyn et al. [2021].

For conceptual simplicity, this work uses a special case of QSVT for Hermitian matrices A , also known as the *quantum eigenvalue transformation*. Matrix functions such as exponentials are more difficult to define for matrices with non-square dimensions and less well-behaved for non-Hermitian matrices with non-real or nonexistent eigenvalues. Cobble is restricted to Hermitian matrices for these existence guarantees to apply; non-Hermitian cases would require different treatment (e.g. dilation to a larger Hermitian operator) and are beyond the immediate scope of this work.

3 EXAMPLE

To illustrate programming in Cobble and reasoning about the costs of programs, in this section we walk through how to express and optimize block-encoded matrices for quantum applications. These examples are loosely derived from the algorithms literature. They are specifically chosen to demonstrate the system and preview the more complex applications we evaluate in Section 7.

3.1 Simulation and Sum Fusion Optimization

Consider the simulation of a system of particles, such as atoms or photons, that permits two distinct operations on pairs of particles. The first operation swaps the energy of two particles, while the

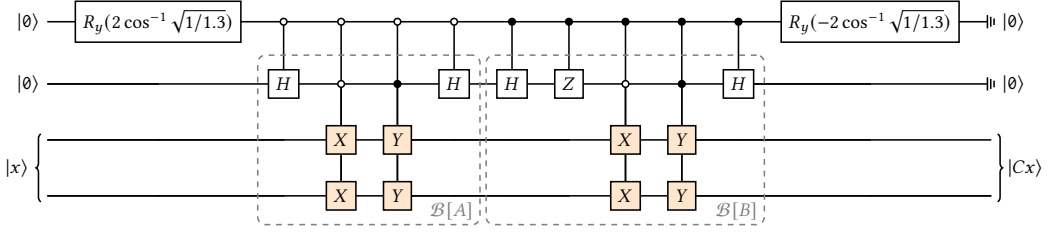


Fig. 1. Quantum circuit to directly implement the system in Equation 3.1, as produced by Cobble. The gates in orange are queries to $\mathcal{B}[X] = X$ and $\mathcal{B}[Y] = Y$. Filled \bullet denotes control on $|1\rangle$ while hollow \circ denotes control on $|0\rangle$. Notation $\text{---}\|$ denotes post-selection: measuring a qubit and starting over until $|0\rangle$ is observed.

```

c = QuantumCircuit(4)
c.ry(2 * arccos(sqrt(1 / 1.3)), 3)
c.append(HGate().control(1, ctrl_state=0), [3, 2])
c.append(MCMTGate(XGate(), 2, 2, ctrl_state='00'), [3, 2, 1, 0])
c.append(MCMTGate(YGate(), 2, 2, ctrl_state='10'), [3, 2, 1, 0])
c.append(HGate().control(1, ctrl_state=0), [3, 2])
c.ch(3, 2)
c.cz(3, 2)
c.append(MCMTGate(XGate(), 2, 2, ctrl_state='01'), [3, 2, 1, 0])
c.append(MCMTGate(YGate(), 2, 2, ctrl_state='11'), [3, 2, 1, 0])
c.ch(3, 2)
c.ry(-2 * arccos(sqrt(1 / 1.3)), 3)

```

Fig. 2. Qiskit code for Figure 1.

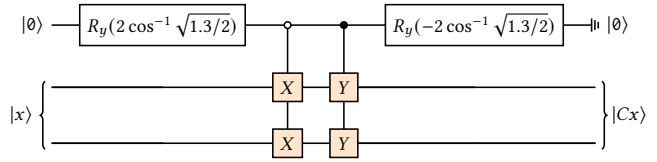


Fig. 3. Optimized circuit for Equation 3.1 after sum fusion.

second excites or suppresses both at once [Roth et al. 2017]. In the form of a *Hamiltonian*, the total energy function of the system, the two operations could be expressed as the 4×4 matrices

$$A = X \otimes X + Y \otimes Y, \quad B = X \otimes X - Y \otimes Y,$$

where $X = \begin{bmatrix} 0 & 1 \\ 1 & 0 \end{bmatrix}$ and $Y = \begin{bmatrix} 0 & -i \\ i & 0 \end{bmatrix}$ coincide with basic single-qubit logic gates. Then, a system that performs A and B simultaneously with relative intensities λ_A and $\lambda_B \in \mathbb{R}$ is a weighted sum

$$C = \lambda_A A + \lambda_B B. \quad (3.1)$$

To find how this system evolves over time, a quantum simulation algorithm [Low and Chuang 2019] multiplies an initial state vector by a function, such as an exponential, of the matrix C . It can then use measurements on the final state to calculate energy or other quantities of interest.

Direct Implementation. To concretely implement this algorithm as a program, a developer must build a block encoding of the matrix C . The developer can express C in Cobble directly according to the mathematical notation above. For parameters $\lambda_A = 1$ and $\lambda_B = 0.3$, the program is:

```

1 X, Y = Basic("X"), Basic("Y")
2 A = kron(X, X) + kron(Y, Y)
3 B = kron(X, X) - kron(Y, Y)
4 C = A + 0.3 * B

```

The Cobble compiler translates this program into the circuit in Figure 1, whose matrix form is $\mathcal{B}[C]$ with scaled C in the top-left block (Definition 2.2). Following the LCU method (Definition 2.4), the circuit first prepares an amplitude encoding of the vector $[\sqrt{1}, \sqrt{0.3}]$ in an *ancilla*, or temporary, qubit. It uses this ancilla to control sub-circuits for $\mathcal{B}[A]$ and $\mathcal{B}[B]$, derived recursively. Finally, it reverses the preparation of the ancilla so that post-selection (see Section 2.2) realizes C .

Using Cobble, the developer need not explicitly list the bit-level rotation and controlled gates in Figure 1 as they would when constructing a quantum circuit in a language such as Qiskit [Javadi-Abhari et al. 2024], depicted for contrast in Figure 2. They can instead use mathematical notation to express an application that compiles, behind the scenes, to a circuit to execute on hardware.

Cost of Direct Implementation. The time complexity of the program is proportional to the number of logic gates in the circuit. Because the precise gate count is implementation-dependent, we may instead count the number of *queries* to the block encodings of the basic matrices that appear in Equation 3.1. Queries are highlighted in Figure 1, where they are basic X and Y logic gates.

The time complexity is also proportional to the *subnormalization* α (see Section 2.2) that scales the encoded C and gives the expected number of repetitions of the circuit until its post-selection succeeds. As stated in Definition 2.4, for the linear combinations A and B we have $\alpha_A = |1| + |1| = 2$ and $\alpha_B = |1| + |-1| = 2$. For C , the subnormalization accumulates as $\alpha_C = \alpha_A + 0.3 \cdot \alpha_B = 2.6$.

Overall, to successfully compute the block encoding of C , the program must execute 8 queries to X and Y per iteration of the circuit and at least 2.6 iterations in expectation, for a total cost of 20.8 queries. Using the Cobble system, the developer can compute these costs automatically:

```
>>> C.queries(), C.subnormalization(), C.total_cost()
(8.0, 2.6, 20.8)
```

Sum Fusion Optimization. The key idea of the *sum fusion* optimization is to flatten the nesting of linear combinations containing negative coefficients that cancel out. In the example,

$$\begin{aligned} C &= 1 \cdot (X \otimes X + Y \otimes Y) + 0.3 \cdot (X \otimes X - Y \otimes Y) \\ &= 1.3 \cdot X \otimes X + 0.7 \cdot Y \otimes Y, \end{aligned}$$

which is equivalent but invokes fewer queries to X and Y and has a lower subnormalization.

Given the original program C , Cobble can automatically perform sum fusion and a set of related rewrites to produce a new program with lower cost. Figure 3 presents the circuit that the Cobble compiler generates after optimization. The optimized program makes only 4 queries to the basic matrices X and Y . It also has a smaller subnormalization $|1.3| + |0.7| = 2.0$, for an overall reduction of $2.6\times$ in total cost. Once again, the Cobble system derives this information automatically:

```
>>> C2 = C.optimize(); (C2.queries(), C2.subnormalization(), C2.total_cost())
(4.0, 2.0, 8.0)
```

3.2 Regression and Polynomial Fusion Optimization

Consider a regression analysis of data measured by a quantum sensor, as could be done in quantum-enhanced learning of physical systems [Huang et al. 2022]. Denoting the dataset as A and the model as B , regression minimizes their error $A - B$. Suppose that for regularization, a quantum regression algorithm [Chakraborty et al. 2023] adapts Huber-like loss functions [Huber 1964] that interpolate between linear and squared error and balance terms that exaggerate or dampen the error:

$$\begin{aligned} f &= (A - B) + \frac{1}{2}(A - B)^2, & g &= (A - B) - \frac{1}{2}(A - B)^2, \\ L &= f \cdot g. \end{aligned} \tag{3.2}$$

The algorithm computes a block encoding of L to find how well the model describes the sensor data. It accesses the dataset via a physical process denoted by a black-box unitary operator $U_A = \mathcal{B}[A]$, and the model via a black-box sub-circuit denoted by a unitary operator $U_B = \mathcal{B}[B]$.

Direct Implementation. Given these black-box inputs, a developer can express L in Cobble following the mathematical notation, and automatically obtain the LCU-based circuit in Figure 4:

```
1 A, B = Basic("U_A", num_ancillas=1), Basic("U_B", num_ancillas=1)
2 f = (A - B) + 1 / 2 * (A - B) ** 2
3 g = (A - B) - 1 / 2 * (A - B) ** 2
4 L = f * g
```

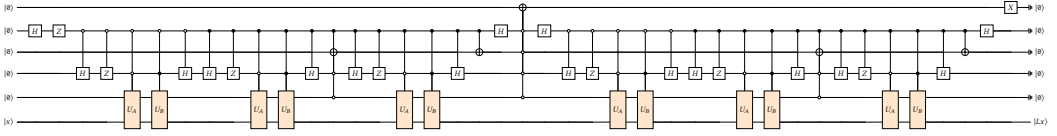


Fig. 4. Quantum circuit to directly implement the function in Equation 3.2, as produced by Cobble. The gates in orange are queries to the black-box operators $\mathcal{B}[A] = U_A$ and $\mathcal{B}[B] = U_B$, assumed to use one ancilla.

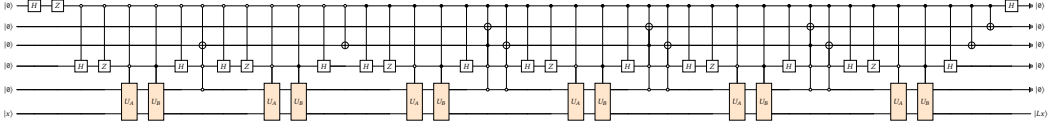


Fig. 5. Intermediate circuit that Cobble produces for Equation 3.2 after sum fusion.

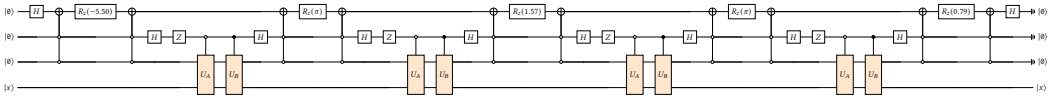


Fig. 6. Optimized circuit that Cobble produces for Equation 3.2 after sum and polynomial fusion.

Sum Fusion. Next, the developer can rewrite the program using sum fusion. Distributing the product and collecting like terms results in a new expression, written compactly as:

$$L = ((A - B) + \frac{1}{2}(A - B)^2) ((A - B) - \frac{1}{2}(A - B)^2) = (A - B)^2 - \frac{1}{4}(A - B)^4.$$

Figure 5 depicts the circuit to which this expression compiles. Notably, sum fusion alone yields little benefit – the new circuit is as complex as Figure 4, despite the new L being more concise. The reason is that for general C and D , the circuit to block-encode $C \cdot D$ sequences the circuits that encode C and D . Figure 5 sequences $A - B$ with itself $2 + 4 = 6$ times for 12 queries in total.

Unlike classical matrix expressions that can be evaluated to a numerical value and cached for reuse, there is no structure-independent mechanism to evaluate a sub-circuit in a quantum block encoding into a form that can be reused cheaply later. Each instance of a matrix must be physically represented by a unitary operator encoding that matrix, whose cost is the same everywhere.

Polynomial Fusion. To make progress, Cobble exploits the structure of the repeated terms in a matrix polynomial. First, it invokes a *polynomial fusion* transformation that merges monomials with the same base and collects polynomial coefficients across the program. Given the program L , Cobble uses the symbolic term $\text{Poly}(X, [a_0, \dots, a_n])$ to denote the polynomial $\sum_{j=0}^n a_j X^j$:

```
>>> f.optimize(), g.optimize()
(Poly((A - B), [0.0, 1.0, 0.5]), Poly((A - B), [0.0, 1.0, -0.5]))
>>> (f * g).optimize() # == L.optimize()
Poly((A - B), [0.0, 0.0, 1.0, 0.0, -0.25])
```

This list of polynomial coefficients is the input required by the quantum singular value transformation (QSVT, Equation 2.5), which can give efficient circuits for suitable polynomials. Cobble first checks and re-scales the coefficients to satisfy the preconditions of Equation 2.5. It next invokes a solver to compute the QSVT rotation angles. Finally, it produces the circuit in Figure 6. Because L has degree 4 and even parity, this circuit makes 4 queries to $A - B$ for a total of 8 queries.

The biggest gain, moreover, is hidden. In the LCU-based implementation from Figure 4, subnormalization is the value of the un-simplified L with absolute values taken for coefficients:

$$\alpha_L^{\text{LCU}} = ((|\alpha_A| + |-\alpha_B|) + \left|\frac{1}{2}\right|(|\alpha_A| + |-\alpha_B|)^2) ((|\alpha_A| + |-\alpha_B|) + \left|-\frac{1}{2}\right|(|\alpha_A| + |-\alpha_B|)^2) = 16,$$

assuming $\alpha_A = \alpha_B = 1$. With the QSVT in Figure 6, it is the *maximum norm* of the simplified L :

$$\alpha_L^{\text{QSVT}} = \max_{-1 \leq x \leq 1} \left| ((\alpha_A + \alpha_B)x)^2 - \frac{1}{4}((\alpha_A + \alpha_B)x)^4 \right| = 1,$$

as Cobble computes automatically. Total cost reduces from $12 \times 16 = 192$ to $8 \times 1 = 8$, a $24\times$ speedup.

4 LANGUAGE

In this section, we present the Cobble language. First, we formalize a core syntax of mathematical operators to manipulate block-encoded matrices, along with its type system and semantics. We then extend this core with a symbolic term that enables the polynomial fusion optimization.

4.1 Core Syntax

The core syntax of Cobble consists of arithmetic operators over block-encoded matrices:

$$\tau ::= \text{bool} \mid \tau_1 \otimes \tau_2$$

$$M ::= \mathcal{B}[A] \mid M^\dagger \mid \lambda_1 M_1 + \lambda_2 M_2 \mid M_1 \cdot M_2 \mid M_1 \oplus M_2 \mid M_1 \otimes M_2 \quad |\lambda_1| + |\lambda_2| > 0$$

where the condition $|\lambda_1| + |\lambda_2| > 0$ prevents division by zero in the denominator of Equation 2.3.

Types. Cobble has Booleans and tensor products, where $\text{bool}^{\otimes n}$ denotes a tuple of n bits. Semantically, an expression has type $\text{bool}^{\otimes n}$ if it encodes an n -qubit matrix of dimension $2^n \times 2^n$. Cobble's type system enforces conditions needed for physical realizability of the generated circuit, such as hermiticity for QSVT (Section 4.3) and consistent subnormalization for direct sums (Section 5.1).

Expressions. The expression $\mathcal{B}[A]$ denotes a black-box block encoding of the matrix A . When A is a standard named gate (e.g., X , Y), the compiler instantiates $\mathcal{B}[A]$ as that gate with no user action. When A is a compound expression (e.g., $B + C$), the compiler recursively decomposes $\mathcal{B}[A]$ into subexpressions. When A is a basic matrix that does not correspond to a single standard gate (e.g., U_A and U_B in Section 3.2), Cobble expects the user to provide the circuit implementing $\mathcal{B}[A]$. Otherwise, the compiler emits a circuit with unevaluated gate names for the user to define.

Other expressions include adjoints, sums, products, and tensor products of block encodings. The choice operator \oplus denotes a *direct sum* of M_1 and M_2 that encodes the two matrices in subspaces distinguished by a Boolean, analogous to a conventional sum type or `if`-expression.

For clarity, the formal syntax and semantics here present binary ($+$, \cdot) rather than n -ary (\sum , \prod) versions of arithmetic operators. The full version of Cobble implemented and studied in subsequent sections provides generalizations to n -ary operators, which we briefly describe below.

Type System. Figure 7 presents the typing rules for the core language of Cobble. A black-box block encoding of a matrix with dimension $2^n \times 2^n$ has type $\text{bool}^{\otimes n}$. The adjoint of an expression has the same type as the original expression. A sum or product of expressions has the type of the summands or factors, provided they have the same type. A direct sum has a Boolean discriminator followed by the type of the summands, subject to a side condition defined in Section 5.1 stating that the summands have equal subnormalization. Finally, a tensor product has product type.

4.2 Semantics

Each well-typed program has an abstract denotational semantics giving the matrix encoded by the program and a concrete compilation semantics giving the circuit that realizes the program.

T-BASE	T-ADJ	T-SUM	T-PRODUCT	T-CHOICE	T-TENSOR
$A \in \mathbb{R}^{2^n \times 2^n}$	$M : \tau$	$M_1 : \tau \quad M_2 : \tau$	$M_1 : \tau \quad M_2 : \tau$	$M_1 : \tau \quad M_2 : \tau \quad \alpha_1 = \alpha_2$	$M_1 : \tau_1 \quad M_2 : \tau_2$
$\mathcal{B}[A] : \text{bool}^{\otimes n}$	$M^\dagger : \tau$	$\lambda_1 M_1 + \lambda_2 M_2 : \tau$	$M_1 \cdot M_2 : \tau$	$M_1 \oplus M_2 : \text{bool} \otimes \tau$	$M_1 \otimes M_2 : \tau_1 \otimes \tau_2$

Fig. 7. Type system of the core language of Cobble. The values λ_1, λ_2 are real scalar literals. In T-CHOICE, α_1 and α_2 are the subnormalizations of M_1 and M_2 ; the side condition $\alpha_1 = \alpha_2$ is defined in Section 5.1.

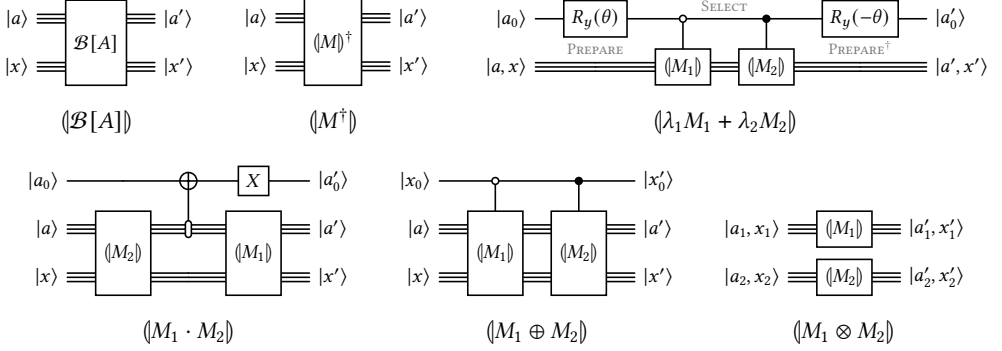


Fig. 8. Compilation semantics of the core language of Cobble.

Denotational Semantics. The denotation $\llbracket M \rrbracket$ is the matrix M encodes, up to subnormalization:

$$\begin{aligned}
\llbracket \mathcal{B}[A] \rrbracket &= A & \llbracket (M^\dagger) \rrbracket &= \llbracket M \rrbracket^\dagger \\
\llbracket \lambda_1 M_1 + \lambda_2 M_2 \rrbracket &= \lambda_1 \llbracket M_1 \rrbracket + \lambda_2 \llbracket M_2 \rrbracket & \llbracket M_1 \cdot M_2 \rrbracket &= \llbracket M_1 \rrbracket \cdot \llbracket M_2 \rrbracket \\
\llbracket M_1 \oplus M_2 \rrbracket &= \llbracket M_1 \rrbracket \oplus \llbracket M_2 \rrbracket & \llbracket M_1 \otimes M_2 \rrbracket &= \llbracket M_1 \rrbracket \otimes \llbracket M_2 \rrbracket
\end{aligned}$$

where \otimes is the Kronecker product and \oplus is the direct sum of matrices, $A \oplus B = \begin{bmatrix} A & 0 \\ 0 & B \end{bmatrix}$.

Compilation Semantics. The circuit $\llbracket M \rrbracket$ is the sequence of logic gates that realizes M in hardware. This circuit operates over two registers, following Equation 2.1: the n -qubit data vector $|x\rangle$ to be multiplied by the encoded matrix and the m -qubit ancilla $|a\rangle$ to be post-selected to all zeroes.

Figure 8 presents the circuit for each operator. The circuit for a black-box block encoding is the block encoding itself, and the circuit for the adjoint of M is the adjoint of the circuit for M .

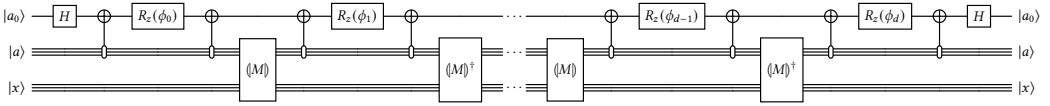
The circuit for addition uses the LCU method of Childs and Wiebe [2012] given in Definition 2.4. To prepare a superposition of the two branches, the circuit performs a rotation on one ancilla qubit by the angle $\theta = 2 \cos^{-1} \sqrt{|\lambda_1| / (|\lambda_1| + |\lambda_2|)}$. The n -ary case would use $\lceil \log n \rceil$ ancilla qubits and a set of controlled rotations. For $\lambda_j < 0$, the circuit adds a Z gate controlled on that branch.

The circuit for multiplication sequentially executes each factor in the conventional reverse order. Following Dalzell et al. [2025]; Sünderhauf [2023], it reuses ancillas between factors and adds one ancilla $|a_0\rangle$ to ensure that all intermediate ancilla states after each factor are post-selected to zero. The n -ary case would add $\lceil \log n \rceil$ ancillas, replace the anti-controlled NOT between factors by an anti-controlled integer increment, and replace the final NOT with a subtraction by $n - 1$.

The circuit for direct sum selects between the circuits for the branches based on the discriminator bit $|x_0\rangle$. It parallels the case for ordinary sum but considers the discriminator as part of the data, which will not be post-selected, rather than the ancilla, which will. Finally, the circuit for tensor product independently executes a circuit for each factor on its data and ancilla components.

$\frac{\text{H-BASE}}{A = A^\dagger} \quad \frac{\text{H-ADJ}}{M = M^\dagger} \quad \frac{\text{H-SUM}}{M_1 = M_1^\dagger \quad M_2 = M_2^\dagger}$	$\frac{\text{H-PRODUCT}}{\llbracket M_1 \rrbracket \llbracket M_2 \rrbracket = \llbracket M_2 \rrbracket \llbracket M_1 \rrbracket \quad M_1 = M_1^\dagger \quad M_2 = M_2^\dagger}$
$\frac{\text{H-CHOICE}}{M_1 = M_1^\dagger \quad M_2 = M_2^\dagger} \quad \frac{\text{H-TENSOR}}{M_1 = M_1^\dagger \quad M_2 = M_2^\dagger} \quad \frac{\text{H-POLY}}{M = M^\dagger}$	$\frac{\text{T-POLY}}{M : \tau \quad M = M^\dagger}$
$\mathcal{B}[A] = (\mathcal{B}[A])^\dagger \quad M^\dagger = M \quad M_1 + M_2 = (M_1 + M_2)^\dagger$	$M_1 \cdot M_2 = (M_1 \cdot M_2)^\dagger$
$M_1 \oplus M_2 = (M_1 \oplus M_2)^\dagger \quad M_1 \otimes M_2 = (M_1 \otimes M_2)^\dagger$	$\text{Poly}(M, p) = \text{Poly}(M, p)^\dagger \quad \text{Poly}(M, p) : \tau$

Fig. 9. Typing rules to check hermiticity and symbolic polynomials. Conditions in gray are user-provided.

Fig. 10. Compilation of a degree- d polynomial using QSVT. Even d is shown; the odd case ends on (M) .

Soundness. The type system is sound with respect to both semantics. Furthermore, the denotational semantics is equal to the sub-matrix in the top-left block of the matrix representation of the compilation semantics, up to rescaling by the subnormalization $\alpha \in \mathbb{R}$ (Definition 2.2).

THEOREM 4.1. *If $M : \tau$, then $\llbracket M \rrbracket$ is a valid matrix and $\langle M \rangle$ is a valid quantum circuit.*

PROOF. By induction on the structure of M . □

THEOREM 4.2. *Assume that $M : \text{bool}^{\otimes n}$ and for all $\mathcal{B}[A] : \text{bool}^{\otimes n_A}$ in M , the $2^{n_A} \times 2^{n_A}$ top-left block of $\mathcal{B}[A]$ is A/α_A for some α_A . Then, the $2^n \times 2^n$ top-left block of $\langle M \rangle$ is $\llbracket M \rrbracket/\alpha$ for some α .*

PROOF. By induction on the structure of M , and invoking the cited prior results. □

4.3 Symbolic Polynomials

We next extend the core language with a symbolic term in the compiler’s intermediate representation that captures matrix polynomials. The compiler rewrites the AST using this term so it can check degree and parity of polynomials and compute QSVT angles to generate a circuit. This term is:

$$M ::= \dots \mid \text{Poly}(M, [a_0, \dots, a_d]) \quad a_j \in \mathbb{R}$$

The denotational semantics of $\text{Poly}(M, [a_0, \dots, a_d])$ is defined to be equal to $\llbracket \sum_{j=0}^d a_j M^j \rrbracket$ in the core language. But when M is Hermitian, i.e. $M = M^\dagger$, the polynomial can be compiled to a more efficient circuit using the quantum singular value transformation as defined in Equation 2.5.

Type System. In Figure 9, we present rules that augment the type system to conservatively check hermiticity of M . For a black-box block encoding $\mathcal{B}[A]$, Cobble requires the user to specify whether A is Hermitian. The adjoint of a Hermitian matrix is Hermitian, as are the sums, direct sums, and tensor products of Hermitian matrices. Products of Hermitian matrices are Hermitian if and only if the factors commute, which Cobble also requires the user to specify. Finally, symbolic polynomials with real coefficients in M are well-typed and Hermitian when M is Hermitian.

Compilation Semantics. Any polynomial $\text{Poly}(M, [a_0, a_1, \dots])$ can be decomposed into even and odd parts $\text{Poly}(M, [a_0, 0, a_2, \dots]) + \text{Poly}(M, [0, a_1, 0, a_3, \dots])$. The QSVT provides an efficient circuit for each part [Lin 2022], depicted in Figure 10. In the circuit, the phase angles ϕ_j are computed from the a_j using a quantum signal processing (QSP) solver such as pyQSP [Martyn et al. 2021].

5 COST MODEL

In this section, we present a cost model provided as an analysis in Cobble that enables the developer to estimate query and subnormalization costs of programs. Building on these principles, we analytically compare the efficiency of different approaches to realize matrix polynomials. The cost model informs optimization decisions in two ways: determining which factoring transformations improve cost and guiding a fallback to other methods should QSVT incur excessive query costs.

5.1 Costs of Core Language

In Table 1, we summarize the runtime costs of each operator in the core language of Cobble. This table combines and generalizes prior results from the theoretical literature, in particular those of Dalzell et al. [2025]; Gilyén et al. [2019]; Harrigan et al. [2024]; Lin [2022].

Queries. The first cost is the number of queries to black-box block encoding oracles, examples of which are X and Y from Section 3.1 and U_A and U_B from Section 3.2. This quantity is proportional to the precise total number of logic gates but less subject to implementation variance. By definition, a black-box block encoding makes one query. Adjoints make the same number of queries as the original expression. For all other operators, the number of queries is the total of the operands.

Subnormalization. The second cost is the subnormalization α of Definition 2.2 that scales the encoded matrix and is proportional to the expected number of circuit repetitions needed to produce the matrix. Black-box terms have subnormalization specified by the user. Adjoints have subnormalization equal to the original expression. Following Definition 2.4, the subnormalization of a sum is the sum of those of the summands, weighted by the absolute value of the coefficients. For products and tensor products, the subnormalization is the product of those of the operands.

Revisiting the rule T-CHOICE for direct sums in Figure 7, a direct sum is only well-defined when the operands have equal subnormalization; the direct sum then takes on that subnormalization. The reason is that $(A/\alpha_1) \oplus (B/\alpha_2) = (A \oplus B)/\alpha$ for some α only when $\alpha_1 = \alpha_2 = \alpha$, a restriction unique to direct sums. The side condition in T-CHOICE thus ensures that a direct sum is well-defined, and the Cobble type checker automatically checks this condition by computing α via Table 1.

Qubits. The third cost is the number of ancilla qubits required to implement the operator. For black-box block encodings, this number is user-specified. For adjoints, it is the same as the original expression. For the other operators, it is the maximum of the number of qubits of the operands. Sums and products also introduce $\lceil \log n \rceil$ selection bits, as discussed in Section 4.2.

Circuit Costs. Though not listed in the table, the total gate count of the computation is the product of the subnormalization, number of queries, and number of gates per query. The last term depends on the implementation of each $\mathcal{B}[A]$, and provides information orthogonal to the other dominant costs in the table. We report concrete gate and qubit counts empirically in Section 7.3.

5.2 Costs of Polynomials

In Table 2, we summarize the cost of implementing $\text{Poly}(M, [a_0, \dots, a_d])$ by four different methods:

- Linear combination of unitaries (LCU, Definition 2.4), which directly evaluates the sum of monomials $\sum_{j=0}^d a_j M^j$ using the core language operators and costs given in Table 1.
- Horner's method, which decomposes $\sum_{j=0}^d a_j M^j = (((a_d M + a_{d-1} I)M + \dots)M + a_0 I)$ and evaluates the polynomial by d iterations of multiplication and addition.
- Quantum singular value transformation (QSVT, Equation 2.5), which constructs the even and odd parts of the polynomial each using the circuit in Figure 10 and takes their sum.

Table 1. Query, subnormalization, and ancilla costs of the core language of Cobble.

Operator	# Queries k	Subnormalization α	# Qubits m
$\mathcal{B}[A]$	1	user-specified	user-specified
M^\dagger	k_M	α_M	m_M
$\sum_{j=1}^n \lambda_j M_j$	$\sum_{j=1}^n k_j$	$\sum_{j=1}^n \lambda_j \alpha_j$	$\lceil \log n \rceil + \max_j m_j$
$\prod_{j=1}^n M_j$	$\sum_{j=1}^n k_j$	$\prod_{j=1}^n \alpha_j$	$\lceil \log n \rceil + \max_j m_j$
$\bigoplus_{j=1}^n M_j$	$\sum_{j=1}^n k_j$	α_j (all equal)	$\max_j m_j$
$\bigotimes_{j=1}^n M_j$	$\sum_{j=1}^n k_j$	$\prod_{j=1}^n \alpha_j$	$\max_j m_j$

Table 2. Worst-case (mixed-parity) costs of implementations of $\text{Poly}(M, p)$ where $p = [a_0, \dots, a_d]$.

Method	# Queries k	Subnormalization α	# Qubits m
LCU	$k_M \sum_{j a_j \neq 0} j$	$\ p(\alpha_M x)\ _1$	$\lceil \log d \rceil + d + m_M$
Horner	$k_M d$	$\ p(\alpha_M x)\ _1$	$2d + m_M$
QSVT	$k_M(2d - 1)$	$\ p_{\text{even}}(\alpha_M x)\ _\infty + \ p_{\text{odd}}(\alpha_M x)\ _\infty$	$2 + m_M$
GQET	$k_M d$	$\ T_p(\alpha_M x)\ _\infty$	$1 + m_M$

- Generalized quantum eigenvalue transformation (GQET) [Sünderhauf 2023], which extends QSVT to mixed-parity polynomials by replacing R_z with arbitrary rotations.

LCU vs. Horner. As shown in the table, the direct implementation by LCU typically requires more queries than the other methods. It makes j queries to M for each monomial M^j in the sum, whereas Horner’s method only makes one query for each of the d iterations. Horner’s method, however, suffers a penalty by incurring two ancillas per iteration – one for the multiplication and one for the addition – whereas LCU performs one sum at the end with only logarithmic cost.

Both methods have the same subnormalization, the ℓ_1 norm of the polynomial coefficients:

$$\|p(\alpha_M x)\|_1 = \sum_{j=0}^d |a_j \alpha_M^j|,$$

and is not affected by the difference in order and factoring of arithmetic operations.

LCU vs. QSVT. Typically, QSVT is more efficient than LCU. For a polynomial with mixed parity $\sum_{j=0}^d a_j M^j$ where a_d and a_{d-1} are both nonzero, the sum of even and odd parts by QSVT makes $d + (d - 1)$ total queries to M , whereas LCU makes that many for M^d and M^{d-1} alone. Moreover, QSVT uses fewer ancillas – one for the circuit in Figure 10 and one for the final sum.

Taking the simplifying assumption that p has fixed parity, the subnormalization for QSVT is equal to the L_∞ (uniform) norm of the polynomial, which is no greater than the ℓ_1 norm:

$$\|p(\alpha_M x)\|_\infty = \max_{-1 \leq x \leq 1} \left| \sum_{j=0}^d a_j \alpha_M^j x^j \right| \leq \|p(\alpha_M x)\|_1$$

by the triangle inequality. It can be much smaller when coefficients a_j have mixed signs.

QSVT vs. GQET. For conceptual completeness, we also compare against the GQET, which generalizes QSVT to mixed-parity polynomials without the need to explicitly split into even and odd parts. It incurs subnormalization equal to the L_∞ norm of the following modified polynomial:

$$\|T_p(\alpha_M x)\|_\infty = \max_{|z|=1} \left| \sum_{j=0}^d a_j T_j(\alpha_M z) \right| \leq O(\log d) \cdot \|p(\alpha_M x)\|_\infty,$$

where $z \in \mathbb{C}$ and $T_j(x)$ is a Chebyshev polynomial of the first kind. This function is non-trivial to compare against the previous cases; [Sünderhauf \[2023\]](#) proves the asymptotic bound above.

5.3 Soundness and Implications

The cost model accurately predicts the costs of the core language and polynomials in Cobble:

THEOREM 5.1. *A well-typed program compiles to a circuit with costs given by Tables 1 and 2.*

PROOF. By induction on the structure of the program. Query and ancilla counts follow directly from the circuits in Figures 8 and 10. Subnormalization for sums, products, and tensor products is proven by [Gilyén et al. \[2019\]](#). Subnormalization for polynomials by LCU and Horner follows by induction. For QSVT, subnormalization follows from the conditions on $P(x)$ in Equation 2.5. \square

The cost model also offers a convenient way to analyze the effect – or lack thereof – of refactoring operators in matrix expressions. Horner’s method refactors the additions and multiplications in a polynomial, which eliminates redundant queries but cannot change the subnormalization.

Section 3.2 illustrates how more general instances of subexpression reuse do not lead to speedup. Absent additional structure of A and B , the expression $(A + B) \cdot (A + B)$ requires two additions, one multiplication, and four total queries to A and B . Exponentiation by squaring is also not admissible in general: $A^{128} = A^{64} \cdot A^{64}$, but squaring A^{64} costs the same as multiplying it by A for 64 times.

6 OPTIMIZATIONS

In this section, we present the optimizations of sum fusion and polynomial fusion in Cobble, along with a set of additional rewrites that enable and complement these optimizations. We show that the system overall is sound, strongly normalizing, and cost-nonincreasing.

6.1 Sum Fusion

The overarching principle of sum fusion is to flatten nested linear combinations of expressions to eliminate intermediate overhead from subnormalization:

$$\sum_k \left(\sum_j a_{k,j} \mathcal{B}[M_j] \right) \mapsto \sum_j \left(\sum_k a_{k,j} \right) \mathcal{B}[M_j]$$

Soundness. Sum fusion preserves the block encoding semantics of the expression, as can be seen by direct algebraic simplification. Note that it does not strictly preserve the compilation semantics.

Cost Reduction. When all coefficients are positive, sum fusion leaves queries and subnormalization unchanged and modestly reduces ancilla count. But when some signs are negative, it can cancel queries and reduce subnormalization by the triangle inequality: $\sum_j |\sum_k a_{k,j}| \leq \sum_k \sum_j |a_{k,j}|$.

The compilation of sums benefits from another practical optimization of merging the subnormalization of each sub-expression with its coefficient. For example, consider the expression $A + 100B$ with $\alpha_A = 100$ and $\alpha_B = 1$. Then, no rotation to prepare $[\sqrt{1}, \sqrt{100}]$ is needed because simply adding the encodings of A and B gives the correct weighted sum where α effectively scales B by 100.

$$\begin{array}{ll}
\text{Poly}(A, f) \cdot \text{Poly}(A, g) \mapsto \text{Poly}(A, f \cdot g) & \text{Poly}(A, f) + \text{Poly}(A, g) \mapsto \text{Poly}(A, f + g) \\
\text{Poly}(A, f) \oplus \text{Poly}(B, f) \mapsto \text{Poly}(A \oplus B, f) & \text{Poly}(\text{Poly}(A, f), g) \mapsto \text{Poly}(A, g \circ f) \\
(A \cdot B) + (A \cdot C) \mapsto A \cdot (B + C) & (B \cdot A) + (C \cdot A) \mapsto (B + C) \cdot A \\
(A \cdot B) \oplus (A \cdot C) \mapsto (I \otimes A) \cdot (B \oplus C) & (B \cdot A) \oplus (C \cdot A) \mapsto (B \oplus C) \cdot (I \otimes A) \\
(A \otimes B) + (A \otimes C) \mapsto A \otimes (B + C) & (B \otimes A) + (C \otimes A) \mapsto (B + C) \otimes A \\
(A \otimes B) \oplus (A \otimes C) \mapsto A \otimes (B \oplus C) & (B \otimes A) \oplus (C \otimes A) \mapsto (B \oplus C) \otimes A \\
A \oplus A \mapsto I \otimes A & A \cdot I \mapsto A & A^\dagger \mapsto A \quad (\text{when } A = A^\dagger) & (A^\dagger)^\dagger \mapsto A \\
(A \cdot B)^\dagger \mapsto B^\dagger \cdot A^\dagger & (A + B)^\dagger \mapsto A^\dagger + B^\dagger & (A \otimes B)^\dagger \mapsto A^\dagger \otimes B^\dagger & (A \oplus B)^\dagger \mapsto A^\dagger \oplus B^\dagger
\end{array}$$

Fig. 11. Selection of additional rewrites that enable and complement sum and polynomial fusion.

6.2 Polynomial Fusion

The overarching principle of polynomial fusion is to merge monomials with the same base expression into symbolic terms that enable more efficient implementation by QSVT:

$$\sum_{j=0}^d a_j M^j \mapsto \text{Poly}(M, [a_0, \dots, a_d])$$

Soundness. Like sum fusion, polynomial fusion preserves the block encoding semantics of the expression (by definition of Poly) but does not strictly preserve the compilation semantics.

Cost Reduction. For all fixed-parity polynomials, fusion into Poly and implementation by QSVT reduce the number of queries to the degree d of the polynomial, whereas in LCU it is greater than d for non-monomials. As shown in Section 5.2, subnormalization reduces to the L_∞ norm, which is no greater than the ℓ_1 norm as in LCU and can be strictly less for mixed-sign coefficients.

QSVT must separate mixed-parity polynomials into even and odd parts, which can increase the number of queries by up to a factor of two over Horner’s method in principle. As we show in Section 7, the improved subnormalization typically outweighs the cost of these queries. Cobble falls back to LCU or Horner’s method otherwise, ensuring that cost is nonincreasing overall.

6.3 Additional Transformations

In Figure 11, we present additional transformations that either expose more opportunities to apply sum and polynomial fusion or eliminate redundant queries from the program. All of the rewrites in the figure are sound by algebraic reasoning on the denotational semantics of Cobble. They never increase the number of queries, and they keep the subnormalization unchanged except when exposing more opportunities for sum and polynomial fusion.

Polynomials. The first few rules simplify symbolic polynomials as much as possible. They merge different polynomials with the same base by multiplying or adding the coefficients, merge direct sums of the same polynomial with different bases by taking the direct sum of the base expressions, and merge nested polynomials by composing the functions given by their coefficients.

Factoring. The next set of rules factor common subexpressions to remove redundant queries. Most originate from matrix algebra, e.g. distributivity of (tensor) products over (direct) sums.

In general, factoring is among the only forms of subexpression reuse that directly improve cost in block encodings. It only applies in limited cases. The example $(A + B) \cdot (A + B)$ from Section 5.3 does not factor into fewer instances of A , whereas $(A \cdot B) + (A \cdot C) = A \cdot (B + C)$ does.

Simplification. The last few rules simplify the expression by pushing down adjoints and eliminating constants. When the type checker finds that a matrix is Hermitian, adjoints can cancel.

Implementation. In Cobble, polynomial discovery is heuristic: the rewrite system does not guarantee that an optimal polynomial form will be found. That said, under a well-founded measure on expressions that strictly decreases under the rules, the rewrite system is strongly normalizing. Supposing the following priority order for rewrites, the system reaches a unique normal form.

In our implementation, optimization proceeds bottom-up, such that subexpressions are optimized first. For sums, rewrites apply in the following order: like terms are flattened, common subexpressions are factored, scalar coefficients are merged into polynomials, polynomials with the same base are combined, and constant terms are merged with polynomials. For products, factors are flattened, polynomial product fusion is applied when possible, and repeated factors are collapsed to Poly.

7 EVALUATION

We implemented Cobble as an embedded language in Python along with a compiler, simulator, and benchmark suite. In this section, we use Cobble to answer the following research questions:

- RQ1.* By how much do the proposed optimizations reduce the cost of matrix expressions?
- RQ2.* Can the Cobble system empirically analyze the costs of known quantum algorithms?
- RQ3.* By how much do existing circuit optimizers reduce the costs of these programs?
- RQ4.* How scalable is the Cobble compiler in compile time with varying problem size?

Implementation. Given a program, the compiler performs type checking (Section 4.1), cost analysis (Section 5), and optimizations (Section 6). It then outputs a quantum circuit in the OpenQASM 2.0 [Cross et al. 2017] format. To solve for QSP phase angles, the compiler invokes pyQSP [Chao et al. 2020; Dong et al. 2021; Martyn et al. 2021] or optionally PennyLane [Bergtholm et al. 2022]. For testing, the simulator invokes Quimb [Gray 2018] to perform classical circuit simulation.

We have released this package as an open-source repository. Moreover, all source code, benchmarks, and experimental scripts are available as part of the software artifact of this paper.

7.1 RQ1: Optimization of Matrix Expressions

RQ1. By how much do the proposed optimizations reduce the cost of matrix expressions?

Benchmarks. This question requires us to establish a set of executable program or circuit benchmarks for the emerging domain of quantum linear algebra applications. We used Cobble to express block encodings of the input matrices corresponding to three applications from the literature:

- *Simulation* (penalized-coupler): a Hamiltonian describing a coupled system subject to a penalty function, which resembles simulation of an Ising model [Cervera-Lierta 2018] or the adiabatic optimization of a constrained satisfaction problem [Farhi et al. 2000].
- *Regression* (ols-ridge): a regularized Gram matrix that interpolates between ordinary least squares [Chakraborty et al. 2023] and ridge regression [Yu et al. 2021] for a model.
- *Image Processing* (laplacian-filter): a two-dimensional Laplacian stencil over a rectangle, as applied in quantum algorithms for edge detection [Fan et al. 2019].

Though some of these applications are not realizable on near-term hardware, they are representative of the design space of the inputs and structure of quantum algorithms for linear algebra, and they test the effectiveness of Cobble for implementing matrix expressions in different domains.

Table 3. Runtime cost comparison for matrix expression benchmarks. Units for cost are # of queries.

Matrix Expression	# Queries \times Subnormalization = Cost		Speedup
	Unoptimized	Optimized	
simulation-example (§ 3.1)	$8 \times 2.6 = 20.8$	$4 \times 2.0 = 8.0$	2.6 \times
regression-example (§ 3.2)	$12 \times 16.0 = 192.0$	$8 \times 1.0 = 8.0$	24.0 \times
penalized-coupler	$6 \times 8.2 = 49.2$	$3 \times 6.2 = 18.6$	2.6 \times
laplacian-filter	$8 \times 59.3 = 474.2$	$2 \times 27.8 = 55.7$	8.5 \times
ols-ridge	$148 \times 529.7 = 7.8e4$	$18 \times 171.5 = 3.1e3$	25.4 \times

Cost Metric. For each benchmark, we computed its runtime cost before and after optimization by the Cobble compiler. We define cost using a formula adapted from Sünderhauf et al. [2024]:

$$\text{Cost} = \# \text{ Queries} \times \text{Subnormalization},$$

where the first term is the number of queries to oracles that encode basic matrices, examples of which are X and Y from Section 3.1 and U_A and U_B from Section 3.2. This number is proportional to the precise count of quantum logic gates in each run of the circuit, which is subject to implementation variance. The second term, subnormalization, is proportional to the number of runs of the circuit required to successfully produce the target matrix through post-selection (Section 2.2).

Results. In Table 3, we present the cumulative effect of the optimizations of Section 6 in terms of runtime cost reduction on each benchmark. The results indicate meaningful speedups under certain settings, ranging from 2.6 \times for the simulation examples to 25.4 \times for the regression examples. Generally, the speedup is larger for longer programs with higher-degree polynomials.

The reported speedups are attributable to the compiler passes proposed in this work: sum fusion and polynomial fusion (and the related rewrites in Section 6), which restructure expressions that would naively compile to nested LCU into compact forms enabling compilation via QSVT.

7.2 RQ2: Resource Analysis of Quantum Algorithms

RQ2. Can the Cobble system empirically analyze the costs of known quantum algorithms?

Benchmarks. For this question, we used Cobble to express block encodings of matrix polynomials that underpin three major quantum algorithms as described by Martyn et al. [2021]:

- *Matrix inversion:* the optimal polynomial approximation by Sünderhauf et al. [2025] for $f(A) = A^{-1}$ in the quantum linear system solver [Childs et al. 2017; Harrow et al. 2009].
- *Hamiltonian simulation:* the Jacobi-Anger decomposition of $f(A) = e^{-iAt}$ in the quantum algorithm to solve the time-dependent Schrödinger equation [Low and Chuang 2019].
- *Spectral thresholding:* the Fourier-Chebyshev expansion of $f(A) = \text{sign}(A) = A(A^2)^{-1/2}$ in quantum search, phase estimation, and eigenvalue filtering [Martyn et al. 2021].

The benchmarks of RQ1 correspond to the input matrices A of these functions $f(A)$. But unlike the input matrices, these $f(A)$ are already assumed by their authors to utilize QSVT for polynomial evaluation, on the basis that QSVT is more efficient than other methods such as LCU. Our evaluation is thus intended to empirically analyze, not surpass, these theoretical claims of efficiency.

Cost Metric. We computed the runtime cost (defined as in RQ1) of each benchmark, using both fusions plus different implementations of polynomials. The first implementation is by linear combination of unitaries (Definition 2.4), and the second is by the quantum singular value transformation

Table 4. Runtime cost comparison for quantum algorithms in Cobble. Each benchmark is a polynomial approximation of a matrix function with given parity, truncated to degree d . Column “LCU” reports a baseline implementation of polynomials using linear combination of unitaries (Definition 2.4), “Horner” reports the use of Horner’s method (Section 5.2), and “QSVT” reports the use of the quantum singular value transform.

Quantum Algorithm	Parity	d	# Queries \times Subnormalization = Cost		
			LCU	Horner	QSVT
Matrix inversion	odd	7	$49 \times 5.2e4 = 2.5e6$	$13 \times 5.2e4 = 6.7e5$	$13 \times 5.4 = 69.8$
Hamiltonian simulation	mixed	10	$120 \times 1.1e3 = 1.3e5$	$15 \times 1.1e3 = 1.6e4$	$29 \times 2.0 = 58.0$
Spectral thresholding	odd	10	$99 \times 5.3e5 = 5.2e7$	$19 \times 5.3e5 = 1.0e7$	$19 \times 2.7 = 51.6$

(Equation 2.5) as intended by the authors of these algorithms. Their difference effectively captures the additional speedup contributed by polynomial fusion via QSVT, versus sum fusion alone.

As another point of comparison, we computed the cost of the polynomial evaluated by Horner’s method as described in Section 5.2. We also evaluated against the GQET from Section 5.2, but its subnormalization and costs for our programs are higher than LCU and are omitted below.

Results. In Table 4, we present the runtime cost for each benchmark and polynomial implementation, as calculated by the Cobble compiler immediately before circuit generation. These results confirm that QSVT is favorable in cost for these benchmarks by several orders of magnitude. They also indicate that subnormalization is the main bottleneck — Horner’s method achieves optimal query count, but its repeated use of arithmetic accumulates a large subnormalization.

Cobble automatically produces the efficient circuits intended by the authors of these algorithms and empirically confirms the theoretical prediction of efficiency of QSVT over LCU. To our knowledge, our system is among the first to achieve this goal for executable quantum programs.

7.3 RQ3: Comparison to Existing Circuit Optimizers

RQ3. By how much do existing circuit optimizers reduce the costs of these programs?

Benchmarks. We used Cobble to compile each unoptimized program above to a quantum circuit in the gate set $\{H, X, \text{CNOT}, R_z(\theta)\}$ of Nam et al. [2018]. For sake of benchmarking, we instantiated each black-box oracle as a random but consistent single-qubit rotation gate. We invoked on each circuit each of these quantum circuit optimizers: Quartz [Xu et al. 2022], wisq [Xu et al. 2025b], Qiskit [Javadi-Abhari et al. 2024], Feynman [Amy et al. 2014], VOQC [Hietala et al. 2021], Pytket [Sivarajah et al. 2020] (peephole and ZX), and QuiZX [QuiZX Developers 2025]. Each optimizer was given input in the Nam gate set, the output of each was confirmed to remain in this gate set, and those that support user-selectable gate sets were explicitly invoked with this gate set.

Cost Metric. We counted the number of qubits and *non-Clifford* gates in the circuits output by each optimizer and the circuits generated by Cobble after the optimizations of Section 6. These counts ignore subnormalization, pretending for simplicity that the circuit only runs once.

A *non-Clifford* gate is not generated by products or tensor products of $\{H, \text{CNOT}, R_z(\pi/2)\}$, and incurs significant overhead under predominant quantum error-correcting codes [Fowler et al. 2012]. In the Nam gate set, the non-Clifford gates are $R_z(\theta)$ with θ not an integral multiple of $\pi/2$.

We chose the Nam gate set because its support for continuous rotations makes it the closest fit for QSVT circuits among standard gate sets supported by existing optimizers. Using the Clifford+ T gate set is an alternative but would be subject to confounding effects. Specifically, the T -count of

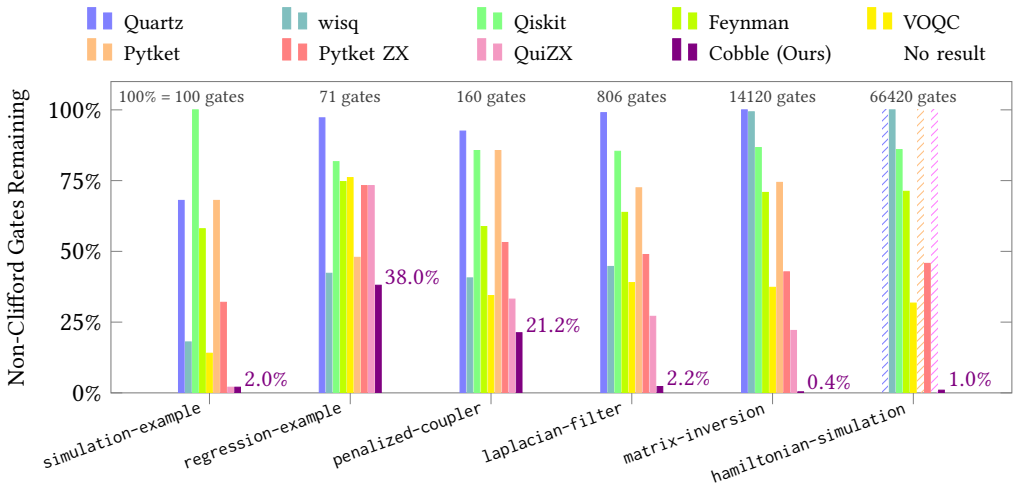


Fig. 12. Gate counts of circuits across benchmarks and optimizers. Each bar shows a normalized fraction of gates of the unoptimized circuit (lower is better). Slashed bars denote optimizers that crashed, used >32 GB of memory, or timed out after one hour. A benchmark is shown if >3 existing optimizers ran to completion.

Table 5. Qubit counts of circuits across benchmarks and optimizers, relative to the unoptimized baseline program. An entry with – indicates that the optimizer did not run to completion to produce a circuit.

Benchmark	# Qubits (% Reduction from Unoptimized Baseline)									
	Base	Quartz	wisq	Qiskit	Feynman	VOQC	Pytket	Pytket ZX	QuiZX	Cobble
simulation-example	5	5 (0%)	5 (0%)	5 (0%)	5 (0%)	5 (0%)	5 (0%)	5 (0%)	5 (0%)	3 (40.0%)
regression-example	6	6 (0%)	6 (0%)	6 (0%)	6 (0%)	6 (0%)	6 (0%)	6 (0%)	6 (0%)	3 (50.0%)
penalized-coupler	7	7 (0%)	7 (0%)	7 (0%)	7 (0%)	7 (0%)	7 (0%)	7 (0%)	7 (0%)	5 (28.6%)
laplacian-filter	11	11 (0%)	11 (0%)	11 (0%)	11 (0%)	11 (0%)	11 (0%)	11 (0%)	11 (0%)	6 (45.5%)
matrix-inversion	12	12 (0%)	12 (0%)	12 (0%)	12 (0%)	12 (0%)	12 (0%)	12 (0%)	12 (0%)	2 (83.3%)
hamiltonian-simulation	16	–	16 (0%)	16 (0%)	16 (0%)	16 (0%)	–	16 (0%)	–	6 (62.5%)
Figure 12 Average		(0%)	(0%)	(0%)	(0%)	(0%)	(0%)	(0%)	(0%)	(51.6%)
ols-ridge	22	–	22 (0%)	22 (0%)	–	–	–	–	–	2 (90.9%)
spectral-thresholding	16	–	16 (0%)	16 (0%)	16 (0%)	–	–	–	–	2 (87.5%)
Overall Average		(0%)	(0%)	(0%)	(0%)	(0%)	(0%)	(0%)	(0%)	(61.0%)

an $R_z(\theta)$ gate is dictated by the specific value of θ as well as the algorithm and tolerance used for the discretization of θ in unitary synthesis – which are not under study in this work.

Results. In Figure 12, we present the comparison of non-Clifford gate counts achieved by different optimizers and Cobble across various benchmarks. Cobble’s optimizations, which operate on high-level program structure rather than circuits, tie or exceed the performance of all of the evaluated circuit optimizers, and its relative performance tends to improve for larger programs.

These results show how specializing compilers to program structure can be useful for complex quantum applications. Circuit optimizers not aware of the algebraic structure of block encodings cannot remove high-level redundancies as easily. They are also restricted by their typical design, which obligates them to strictly (or very closely) preserve the semantics of the input circuit. By contrast, sum and polynomial fusion reduce subnormalization – preserving the block encoding semantics (Section 4.2) but not the overly conservative circuit semantics of the program.

With that said, a developer can benefit from invoking sum and polynomial fusion in Cobble followed by an existing circuit optimizer to obtain orthogonal and compounding improvements. For hamiltonian-simulation, the additional gate reduction from running a circuit optimizer on the output of Cobble ranges from 12.8% (Qiskit) to 86.0% (QuiZX). The other programs in Figure 12 become too small after sum and polynomial fusion to permit meaningful comparison.

Our results show that existing circuit optimizers do not change the qubit usage for the programs in Figure 12, whereas Cobble reduces it by an average of 52% (see Table 5; 29% for penalized-coupler up to 83% for matrix-inversion). Because the specific circuits analyzed here are mainly bottlenecked by gates and not qubits, this reduction is not a primary emphasis of our study.

7.4 RQ4: Scalability in Compile Time

RQ4. How scalable is the Cobble compiler in compile time with varying problem size?

Benchmarks. For this research question, we implemented a family of programs that block-encode the Chebyshev polynomials $T_n(A)$, which scale uniformly for testing, for $2 \leq n \leq 30$. We executed the Cobble compiler on each program with all optimizations enabled and with pyQSP as the external solver. We measured the time taken to produce a circuit as the average of 10 samples. All timing results were collected on a 2.4 GHz Intel Core i9 processor.

Results. In Figure 13, we present how the compile time used by Cobble scales with the gate count of the unoptimized program. As shown in the graph, Cobble can process and optimize a high-level program whose unoptimized circuit would contain millions of logic gates, in a fraction of a second. Much of the time is spent in a single call to the external numerical solver for QSP phase angles from polynomial coefficients, a computationally intensive step [Dong et al. 2021] reported as a separate component of the total. Cobble’s compilation speed could be directly improved by reducing overhead from the QSP solver or from the Python interpreter.

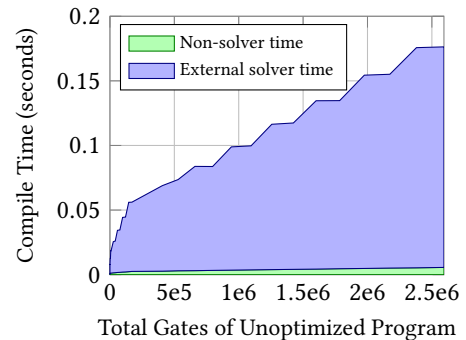


Fig. 13. Compile time taken by Cobble using the pyQSP external solver. The standard error of the mean is less than 0.001 seconds throughout.

8 LIMITATIONS AND NEXT STEPS

In this section, we discuss current limitations of Cobble and opportunities for future work.

Basic Matrix Encodings. Cobble currently asks a user to provide block encodings for basic matrices, which range from trivial unitary gates to potentially complex sub-circuits, before composing them via arithmetic operators. Basic matrices are where compositionality appears to end and case-by-case reasoning must begin. An important next step is to design and provide abstractions for known matrix structures, such as banded, circulant, and Toeplitz matrices, from the literature [Camps et al. 2024; Camps and Van Beeumen 2022; Sünderhauf et al. 2024]. A long-term goal is to develop domain-specific languages for a broader range of matrix structures relevant to applications.

Commutativity. Cobble currently asks a user to specify whether a product of matrices commutes. Automatic checking of this condition is a hard problem today in circuit optimization, since commutativity is not an inductively defined property on matrices and numerical evaluation is not scalable. A first step toward more automation is to hard-code important cases, such as the product of Pauli matrices. A longer term solution could be to analyze the algebraic structure of matrices using tools from representation theory or the ZX-calculus [Coecke and Duncan 2011].

Rewrite Rules. Cobble currently uses a set of manually implemented rewrites that invite exploration of completeness or automation. This understanding must be grounded in new benchmarks, which are still emerging. Initial steps, however, include systematically applying rules via equality saturation [Tate et al. 2011] and verifying rules via proof assistants [Liu et al. 2022]. In the longer term, program synthesis [Xu et al. 2023] could help discover new rules automatically.

Approximation. Like many other compilers, Cobble does not fully account for the approximation inherent in quantum algorithms, whose cost must be calculated and traded off to execute programs on resource-constrained hardware such as near-term noisy devices or emerging error-correcting codes. A step toward better error and cost analysis is to formalize in the language the precision parameter ϵ of block encodings. In the longer term, methods such as those of Hung et al. [2019] could help track error in QSP phase calculation, λ state preparation, and R_z synthesis.

9 RELATED WORK

In this section, we survey the research that is most closely relevant to this work.

Quantum Programming Languages. Researchers have developed many languages for expressing, analyzing, and verifying quantum algorithms. Recent ideas in language design beyond circuits include automatic uncomputation [Bichsel et al. 2020], pointers and memory [Yuan and Carbin 2022], classical effects [Voichick et al. 2023], control flow in superposition [Yuan et al. 2024], type systems for basis [Adams et al. 2025], and call stacks for recursion [Zhang and Ying 2025].

Other work in the community has led to more effective compilers for quantum programs [Huang and Palsberg 2024; Peduri et al. 2022; Peng et al. 2024; Sharma and Achour 2025; Tornow et al. 2025] as well as more robust verification tools [Chen et al. 2023; Huang et al. 2025; Xu et al. 2025a].

Our work introduces a new programming abstraction targeting a new domain — mathematical operators for block encodings in quantum computational linear algebra. We hope these insights will lead to languages that enable developers to realize broader classes of algorithms.

Quantum Resource Estimation. Parallel to the design of languages and compilers is the creation of quantum resource estimation frameworks such as Qualtran [Harrigan et al. 2024], Bartiq [PsiQuantum Team 2024], Azure QRE [van Dam et al. 2023], and pyLIQTR [Obenland et al. 2025]. Given a complex algorithm that is hard to compile directly, these frameworks typically emphasize the ability to produce practical hardware cost estimates rather than explicit executable circuits.

Our work can help in developing these frameworks, which have emerging support for quantum linear algebra, into more full-fledged compilers. We build on prior work on Qualtran [Harrigan et al. 2024] that observed a limited case of sum fusion by formalizing the general technique in a language with sound semantics and evaluating it across a broad set of benchmarks.

Quantum Singular Value Transformation. Block encodings and the QSVT culminate a long line of research in quantum linear algebra. They generalize prior representations of matrices in algorithms for simulation [Low and Chuang 2019] and matrix inversion [Childs et al. 2017], while unifying these tasks with search and phase estimation [Martyn et al. 2021]. Given that more general assumptions of unstructured matrix access can erase quantum speedup [Tang 2019], block encodings define the structure of matrices that are relevant and efficient to encode into a quantum computer.

Interest in the QSVT has led to new numerical solvers for QSP phase angles [Alexis et al. 2026; Berntson and Sünderhauf 2025; Dong et al. 2021], adaptation to mixed-parity polynomials [Motlagh and Wiebe 2024; Sünderhauf 2023], and even hardware realization [Kikuchi et al. 2023]. Procedures to build the QSVT circuit (Figure 10) from an input list of phase angles have recently been added to the PennyLane [Bergholm et al. 2022] and Qmod [Vax et al. 2025] programming frameworks.

Our work provides a roadmap to deploy this mathematical toolkit: a high-level language and compiler that instantiate and test existing solvers and circuit constructions, a type system that checks required conditions for QSVT matrices and polynomials, and an empirical comparison of QSVT against other methods to evaluate where it gives the biggest gains in practice.

Classical Linear Algebra. Ever since BLAS [Blackford et al. 2002] and LAPACK [Anderson et al. 1990], linear algebra has been central in programming, compilers, and high-performance computing. Researchers have developed numerous methods [Anzt et al. 2022; Frigo and Johnson 2005; Kjolstad et al. 2017; Puschel et al. 2005; Tomov et al. 2010; Van Zee et al. 2009; Whaley and Dongarra 1998] to automatically tailor linear algebra to workloads and architectures. Machine learning has further accelerated interest in practical and scalable compilers [Abadi et al. 2016; Chen et al. 2018; Frostig et al. 2018; Paszke et al. 2019; Sabne 2020]. Of these tools, perhaps the closest analogue to Cobble is Eigen [Guennebaud et al. 2010], a user-facing library and optimizer for matrix expressions.

Our work takes a step toward similar goals in expressing and optimizing quantum algorithms. It also suggests that our assumptions about how to optimize programs, such as computation graphs that rely on unrestricted sharing of subexpressions, should be revisited in the quantum world.

10 CONCLUSION

Modern quantum algorithms for linear algebra constitute many of our hopes to reap the reward of practical computational advantage from our investment into hardware quantum devices. Like an intricate puzzle, they present new challenges – building and optimizing complex programs – and new insights that change the way we think about and interact with computation.

In this work, we present high-level programming abstractions for quantum linear algebra, which we hope will help unlock this rare domain of potentially exponential speedup. Through the sum and polynomial fusion optimizations, we also hope to catalyze the discovery of powerful structural rewrites analogous to loop-invariant code motion and strength reduction from classical compilers. And by building systems that reduce need for expert-level reasoning about qubits and logic gates, we hope to eventually enable a broad range of programmers to use a quantum computer.

ACKNOWLEDGMENTS

We thank Isaac Chuang and Patrick Rall for providing an introduction to the theory and applications of block encodings. We thank Matthew Harrigan for providing an environment to explore related ideas and Anurudh Peduri for invaluable technical discussions. We thank Swamit Tannu and Aws Albarghouthi for feedback on drafts of this work. We thank the Center for High-Throughput Computing at the University of Wisconsin–Madison for providing computational resources. Support for this research was provided by the Office of the Vice Chancellor for Research at the University of Wisconsin–Madison with funding from the Wisconsin Alumni Research Foundation.

DATA AVAILABILITY STATEMENT

The artifact for this paper, including source code, benchmark programs, and evaluation package, is available on Zenodo [Yuan 2026].

REFERENCES

- Martín Abadi, Paul Barham, Jianmin Chen, Zhifeng Chen, Andy Davis, Jeffrey Dean, Matthieu Devin, Sanjay Ghemawat, Geoffrey Irving, Michael Isard, Manjunath Kudlur, Josh Levenberg, Rajat Monga, Sherry Moore, Derek G. Murray, Benoit Steiner, Paul Tucker, Vijay Vasudevan, Pete Warden, Martin Wicke, Yuan Yu, and Xiaoqiang Zheng. 2016. TensorFlow: a system for large-scale machine learning. In *USENIX Conference on Operating Systems Design and Implementation*. doi:10.48550/arXiv.1605.08695

- Austin J. Adams, Sharjeel Khan, Arjun S. Bhamra, Ryan R. Abusaada, Jeffrey S. Young, and Thomas M. Conte. 2025. Qwerty: A Basis-Oriented Quantum Programming Language. arXiv:2404.12603 [quant-ph] doi:10.48550/arXiv.2404.12603
- Michel Alexis, Lin Lin, Gevorg Mnatsakanyan, Christoph Thiele, and Jiasu Wang. 2026. Infinite quantum signal processing for arbitrary Szegő functions. *Communications on Pure and Applied Mathematics* 79 (2026). doi:10.1002/cpa.70007
- Matthew Amy, Dmitri Maslov, and Michele Mosca. 2014. Polynomial-Time T-Depth Optimization of Clifford+T Circuits Via Matroid Partitioning. *IEEE Transactions on Computer-Aided Design of Integrated Circuits and Systems* 33, 10 (2014). doi:10.1109/TCAD.2014.2341953
- E. Anderson, Z. Bai, Jack Dongarra, A. Greenbaum, A. McKenney, J. Du Croz, S. Hammarling, James Demmel, C. Bischof, and D. Sorensen. 1990. LAPACK: a portable linear algebra library for high-performance computers. In *ACM/IEEE Conference on Supercomputing*. doi:10.1109/SUPERC.1990.129995
- Hartwig Anzt, Terry Cojean, Goran Flegar, Fritz Göbel, Thomas Grützmacher, Pratik Nayak, Tobias Ribizel, Yuhsiang Mike Tsai, and Enrique S. Quintana-Ortí. 2022. Ginkgo: A Modern Linear Operator Algebra Framework for High Performance Computing. *ACM Trans. Math. Software* 48, 1 (2022). doi:10.1145/3480935
- Ryan Babbush, Craig Gidney, Dominic W. Berry, Nathan Wiebe, Jarrod R. McClean, Alexandru Paler, Austin G. Fowler, and Hartmut Neven. 2018. Encoding Electronic Spectra in Quantum Circuits with Linear T Complexity. *Physical Review X* 8, 4 (2018). doi:10.1103/PhysRevX.8.041015
- Ville Bergholm, Josh Izaac, Maria Schuld, Christian Gogolin, Shah Nawaz Ahmed, Vishnu Ajith, M. Sohaib Alam, Guillermo Alonso-Linaje, B. AkashNarayanan, Ali Asadi, Juan Miguel Arrazola, Utkarsh Azad, Sam Banning, Carsten Blank, Thomas R Bromley, Benjamin A. Cordier, et al. 2022. PennyLane: Automatic differentiation of hybrid quantum-classical computations. arXiv:1811.04968 [quant-ph] doi:10.48550/arXiv.1811.04968
- Bjorn K. Berntson and Christoph Sünnerhauf. 2025. Complementary Polynomials in Quantum Signal Processing. *Communications in Mathematical Physics* 406, 7 (2025). doi:10.1007/s00220-025-05302-9
- Dominic W. Berry. 2014. High-order quantum algorithm for solving linear differential equations. *Journal of Physics A: Mathematical and Theoretical* 47 (2014). doi:10.1088/1751-8113/47/10/105301
- Dominic W. Berry, Andrew M. Childs, Richard Cleve, Robin Kothari, and Rolando D. Somma. 2014. Exponential improvement in precision for simulating sparse Hamiltonians. In *ACM Symposium on Theory of Computing*. doi:10.1145/2591796.2591854
- Benjamin Bichsel, Maximilian Baader, Timon Gehr, and Martin Vechev. 2020. Silq: A High-Level Quantum Language with Safe Uncomputation and Intuitive Semantics. In *ACM SIGPLAN Conference on Programming Language Design and Implementation*. doi:10.1145/3385412.3386007
- L. Susan Blackford, Antoine Petitet, Roldan Pozo, Karin Remington, R. Clint Whaley, James Demmel, Jack Dongarra, Iain Duff, Sven Hammarling, Greg Henry, et al. 2002. An updated set of basic linear algebra subprograms (BLAS). *ACM Trans. Math. Software* 28, 2 (2002). doi:10.1145/567806.567807
- Dolev Bluvstein, Simon J. Evered, Alexandra A. Geim, Sophie H. Li, Hengyun Zhou, Tom Manovitz, Sepehr Ebadi, Madelyn Cain, Marcin Kalinowski, Dominik Hangleiter, J. Pablo Bonilla Ataides, Nishad Maskara, Iris Cong, Xun Gao, Pedro Sales Rodriguez, Thomas Karolyshyn, Giulia Semeghini, Michael J. Gullans, Markus Greiner, Vladan Vuletić, and Mikhail D. Lukin. 2023. Logical quantum processor based on reconfigurable atom arrays. *Nature* 626 (2023). doi:10.1038/s41586-023-06927-3
- Daan Camps, Lin Lin, Roel Van Beeumen, and Chao Yang. 2024. Explicit Quantum Circuits for Block Encodings of Certain Sparse Matrices. *SIAM J. Matrix Anal. Appl.* 45, 1 (2024). doi:10.1137/22M1484298
- Daan Camps and Roel Van Beeumen. 2022. FABLE: Fast Approximate Quantum Circuits for Block-Encodings. In *IEEE International Conference on Quantum Computing and Engineering*. doi:10.1109/qce53715.2022.00029
- Alba Cervera-Lierta. 2018. Exact Ising model simulation on a quantum computer. *Quantum* 2 (2018). doi:10.22331/q-2018-12-21-114
- Shantanav Chakraborty, Aditya Morolia, and Anurudh Peduri. 2023. Quantum Regularized Least Squares. *Quantum* 7 (2023). doi:10.22331/q-2023-04-27-988
- Rui Chao, Dawei Ding, Andrés Gilyén, Cupjin Huang, and Mario Szegedy. 2020. Finding Angles for Quantum Signal Processing with Machine Precision. (2020). arXiv:2003.02831 [quant-ph] doi:10.48550/arXiv.2003.02831
- Tianqi Chen, Thierry Moreau, Ziheng Jiang, Lianmin Zheng, Eddie Yan, Meghan Cowan, Haichen Shen, Leyuan Wang, Yuwei Hu, Luis Ceze, Carlos Guestrin, and Arvind Krishnamurthy. 2018. TVM: an automated end-to-end optimizing compiler for deep learning. In *USENIX Conference on Operating Systems Design and Implementation*.
- Yu-Fang Chen, Kai-Min Chung, Ondřej Lengál, Jyun-Ao Lin, Wei-Lun Tsai, and Di-De Yen. 2023. An Automata-Based Framework for Verification and Bug Hunting in Quantum Circuits. In *ACM SIGPLAN Conference on Programming Language Design and Implementation*. doi:10.1145/3591270
- Andrew M. Childs, Robin Kothari, and Rolando D. Somma. 2017. Quantum Algorithm for Systems of Linear Equations with Exponentially Improved Dependence on Precision. *SIAM J. Comput.* 46, 6 (2017). doi:10.1137/16m1087072
- Andrew M. Childs and Nathan Wiebe. 2012. Hamiltonian Simulation Using Linear Combinations of Unitary Operations. *Quantum Information and Computation* 12 (2012). doi:10.26421/qic12.11-12

- Bob Coecke and Ross Duncan. 2011. Interacting quantum observables: categorical algebra and diagrammatics. *New Journal of Physics* 13, 4 (2011). doi:10.1088/1367-2630/13/4/043016
- Andrew W. Cross, Lev S. Bishop, John A. Smolin, and Jay M. Gambetta. 2017. Open Quantum Assembly Language. arXiv:1707.03429 [quant-ph] doi:10.48550/arXiv.1707.03429
- Alexander M. Dalzell, Sam McArdle, Mario Berta, Przemyslaw Bienias, Chi-Fang Chen, András Gilyén, Connor T. Hann, Michael J. Kastoryano, Emil T. Khabiboulline, Aleksander Kubica, Grant Salton, Samson Wang, and Fernando G. S. L. Brandão. 2025. *Quantum Algorithms: A Survey of Applications and End-to-end Complexities*. Cambridge University Press. doi:10.1017/9781009639651
- Yulong Dong, Xiang Meng, K. Birgitta Whaley, and Lin Lin. 2021. Efficient phase-factor evaluation in quantum signal processing. *Physical Review A* 103, 4 (2021). doi:10.1103/physreva.103.042419
- Ping Fan, Ri-Gui Zhou, Wen Wen Hu, and NaiHuan Jing. 2019. Quantum image edge extraction based on Laplacian operator and zero-cross method. *Quantum Information Processing* 18 (2019). doi:10.1007/s11128-018-2129-x
- Edward Farhi, Jeffrey Goldstone, Sam Gutmann, and Michael Sipser. 2000. Quantum Computation by Adiabatic Evolution. arXiv:quant-ph/0001106 [quant-ph] doi:10.48550/arXiv.quant-ph/0001106
- Austin G. Fowler, Matteo Mariantoni, John M. Martinis, and Andrew N. Cleland. 2012. Surface codes: Towards practical large-scale quantum computation. *Physical Review A* 86, 3 (2012). doi:10.1103/PhysRevA.86.032324
- M. Frigo and S.G. Johnson. 2005. The Design and Implementation of FFTW3. *Proc. IEEE* 93, 2 (2005). doi:10.1109/JPROC.2004.840301
- Roy Frostig, Matthew Johnson, and Chris Leary. 2018. Compiling machine learning programs via high-level tracing. In *Systems for Machine Learning*.
- András Gilyén, Yuan Su, Guang Hao Low, and Nathan Wiebe. 2019. Quantum singular value transformation and beyond: exponential improvements for quantum matrix arithmetics. In *ACM Symposium on Theory of Computing*. doi:10.1145/3313276.3316366
- Google Quantum AI. 2025. Quantum error correction below the surface code threshold. *Nature* 638 (2025). doi:10.1038/s41586-024-08449-y
- Johnnie Gray. 2018. quimb: A python package for quantum information and many-body calculations. *Journal of Open Source Software* 3, 29 (2018). doi:10.21105/joss.00819
- Gaël Guennebaud, Benoît Jacob, et al. 2010. Eigen v3. <http://eigen.tuxfamily.org>.
- Lukas Hantzko, Lennart Binkowski, and Sabhyata Gupta. 2024. Tensorized Pauli decomposition algorithm. *Physica Scripta* 99, 8 (2024). doi:10.1088/1402-4896/ad6499
- Matthew Harrigan, Tanuj Khattar, Charles Yuan, Anurudh Peduri, Noureldin Yosri, Fionn D. Malone, Ryan Babbush, and Nicholas C. Rubin. 2024. Expressing and Analyzing Quantum Algorithms with Qualtran. arXiv:2409.04643 [quant-ph] doi:10.48550/arXiv.2409.04643
- Aram W. Harrow, Avinatan Hassidim, and Seth Lloyd. 2009. Quantum Algorithm for Linear Systems of Equations. *Physical Review Letters* 103, 15 (2009). doi:10.1103/PhysRevLett.103.150502
- Kesha Hietala, Robert Rand, Shih-Han Hung, Xiaodi Wu, and Michael Hicks. 2021. A Verified Optimizer for Quantum Circuits. In *ACM SIGPLAN Symposium on Principles of Programming Languages*. doi:10.1145/3434318
- Hsin-Yuan Huang, Michael Broughton, Jordan Cotler, Sitan Chen, Jerry Li, Masoud Mohseni, Hartmut Neven, Ryan Babbush, Richard Kueng, John Preskill, and Jarrod R. McClean. 2022. Quantum advantage in learning from experiments. *Science* 376, 6598 (2022). doi:10.1126/science.abn7293
- Keli Huang and Jens Palsberg. 2024. Compiling Conditional Quantum Gates without Using Helper Qubits. In *ACM SIGPLAN Conference on Programming Language Design and Implementation*. doi:10.1145/3656436
- Qifan Huang, Li Zhou, Wang Fang, Mengyu Zhao, and Mingsheng Ying. 2025. Efficient Formal Verification of Quantum Error Correcting Programs. In *ACM SIGPLAN Conference on Programming Language Design and Implementation*. doi:10.1145/3729293
- Peter J. Huber. 1964. Robust Estimation of a Location Parameter. *The Annals of Mathematical Statistics* 35, 1 (1964). doi:10.1214/aoms/1177703732
- Shih-Han Hung, Kesha Hietala, Shaopeng Zhu, Mingsheng Ying, Michael Hicks, and Xiaodi Wu. 2019. Quantitative Robustness Analysis of Quantum Programs. In *ACM SIGPLAN Symposium on Principles of Programming Languages*. doi:10.1145/3290344
- Ali Javadi-Abhari, Matthew Treinish, Kevin Krsulich, Christopher J. Wood, Jake Lishman, Julien Gacon, Simon Martiel, Paul D. Nation, Lev S. Bishop, Andrew W. Cross, Blake R. Johnson, and Jay M. Gambetta. 2024. Quantum computing with Qiskit. arXiv:2405.08810 [quant-ph] doi:10.48550/arXiv.2405.08810
- Yuta Kikuchi, Conor Mc Keever, Luuk Coopmans, Michael Lubasch, and Marcello Benedetti. 2023. Realization of quantum signal processing on a noisy quantum computer. *npj Quantum Information* 9 (2023). doi:10.1038/s41534-023-00762-0
- Fredrik Kjolstad, Shoab Kamil, Stephen Chou, David Lugato, and Saman Amarasinghe. 2017. The Tensor Algebra Compiler. In *ACM SIGPLAN Conference on Object-Oriented Programming, Systems, Languages, and Applications*. doi:10.1145/3133901

- Haoya Li, Hongkang Ni, and Lexing Ying. 2023. On efficient quantum block encoding of pseudo-differential operators. *Quantum* 7 (2023). doi:10.22331/q-2023-06-02-1031
- Lin Lin. 2022. Lecture Notes on Quantum Algorithms for Scientific Computation. arXiv:2201.08309 [quant-ph] doi:10.48550/arXiv.2201.08309
- Amanda Liu, Gilbert Louis Bernstein, Adam Chlipala, and Jonathan Ragan-Kelley. 2022. Verified Tensor-Program Optimization Via High-Level Scheduling Rewrites. In *ACM SIGPLAN Symposium on Principles of Programming Languages*. doi:10.1145/3498717
- Guang Hao Low and Isaac L. Chuang. 2019. Hamiltonian Simulation by Qubitization. *Quantum* 3 (2019). doi:10.22331/q-2019-07-12-163
- Guang Hao Low, Vadym Kliuchnikov, and Luke Schaeffer. 2024. Trading T gates for dirty qubits in state preparation and unitary synthesis. *Quantum* 8 (2024). doi:10.22331/q-2024-06-17-1375
- John M. Martyn, Zane M. Rossi, Andrew K. Tan, and Isaac L. Chuang. 2021. Grand Unification of Quantum Algorithms. *PRX Quantum* 2, 4 (2021). doi:10.1103/prxquantum.2.040203
- Danial Motlagh and Nathan Wiebe. 2024. Generalized Quantum Signal Processing. *PRX Quantum* 5 (2024). doi:10.1103/PRXQuantum.5.020368
- Yunseong Nam, Neil J. Ross, Yuan Su, Andrew M. Childs, and Dmitri Maslov. 2018. Automated optimization of large quantum circuits with continuous parameters. *npj Quantum Information* 4, 1 (2018). doi:10.1038/s41534-018-0072-4
- Martina Nibbi and Christian B. Mendl. 2024. Block encoding of matrix product operators. *Physical Review A* 110, 4 (2024). doi:10.1103/physreva.110.042427
- Michael A. Nielsen and Isaac L. Chuang. 2010. *Quantum Computation and Quantum Information* (10th ed.). Cambridge University Press, New York. doi:10.1017/CBO9780511976667
- Kevin Obenland, Justin Elenewski, Kaitlyn Morrell, Benjamin Rempfer, Parker Kuklinski, Rylee Stuart Neumann, Arthur Kurlej, Robert Rood, John Blue, and Joe Belarge. 2025. *pyLIQTR*. doi:10.5281/zenodo.16794505
- Adam Paszke, Sam Gross, Francisco Massa, Adam Lerer, James Bradbury, Gregory Chanan, Trevor Killeen, Zeming Lin, Natalia Gimelshein, Luca Antiga, Alban Desmaison, Andreas Köpf, Edward Yang, Zach DeVito, Martin Raison, Alykhan Tejani, Sasank Chilamkurthy, Benoit Steiner, Lu Fang, Junjie Bai, and Soumith Chintala. 2019. *PyTorch: an imperative style, high-performance deep learning library*. doi:10.48550/arXiv.1912.01703
- Anurudh Peduri, Siddharth Bhat, and Tobias Grosser. 2022. QSSA: An SSA-Based IR for Quantum Computing. In *ACM SIGPLAN International Conference on Compiler Construction*. doi:10.1145/3497776.3517772
- Yuxiang Peng, Jacob Young, Pengyu Liu, and Xiaodi Wu. 2024. SimuQ: A Framework for Programming Quantum Hamiltonian Simulation with Analog Compilation. In *ACM SIGPLAN Symposium on Principles of Programming Languages*. doi:10.1145/3632923
- PsiQuantum Team. 2024. Bartiq. <https://github.com/PsiQ/bartiq>
- M. Puschel, J.M.F. Moura, J.R. Johnson, D. Padua, M.M. Veloso, B.W. Singer, Jianxin Xiong, F. Franchetti, A. Gacic, Y. Voronenko, K. Chen, R.W. Johnson, and N. Rizzolo. 2005. SPIRAL: Code Generation for DSP Transforms. *Proc. IEEE* 93, 2 (2005). doi:10.1109/JPROC.2004.840306
- QuiZX Developers. 2025. QuiZX: a quick Rust port of PyZX. <https://github.com/zxcalc/quizz>
- Marco Roth, Marc Ganzhorn, Nikolaj Moll, Stefan Filipp, Gian Salis, and Sebastian Schmidt. 2017. Analysis of a parametrically driven exchange-type gate and a two-photon excitation gate between superconducting qubits. *Physical Review A* 96, 6 (2017). doi:10.1103/physreva.96.062323
- Amit Sabne. 2020. XLA: Compiling Machine Learning for Peak Performance.
- Artur Scherer, Benoît Valiron, Siun-Chuon Mau, Scott Alexander, Eric van den Berg, and Thomas E. Chapuran. 2017. Concrete resource analysis of the quantum linear-system algorithm used to compute the electromagnetic scattering cross section of a 2D target. *Quantum Information Processing* 16 (2017). doi:10.1007/s11128-016-1495-5
- Ritvik Sharma and Sara Achour. 2025. Optimizing Ancilla-Based Quantum Circuits with SPARE. In *ACM SIGPLAN Conference on Programming Language Design and Implementation*. doi:10.1145/3729253
- Seyon Sivarajah, Silas Dilkes, Alexander Cowtan, Will Simmons, Alec Edgington, and Ross Duncan. 2020. t[ket]: a retargetable compiler for NISQ devices. *Quantum Science and Technology* 6, 1 (2020). doi:10.1088/2058-9565/ab8e92
- Krysta M. Svore, Martin Roetteler, Alan Geller, Matthias Troyer, John Azariah, Christopher Granade, Bettina Heim, Vadym Kliuchnikov, Mariia Mykhailova, and Andres Paz. 2018. Q#: Enabling Scalable Quantum Computing and Development with a High-level DSL. In *Real World Domain Specific Languages Workshop*. doi:10.1145/3183895.3183901
- Christoph Sünderhauf. 2023. Generalized Quantum Singular Value Transformation. arXiv:2312.00723 [quant-ph] doi:10.48550/arXiv.2312.00723
- Christoph Sünderhauf, Earl Campbell, and Joan Camps. 2024. Block-encoding structured matrices for data input in quantum computing. *Quantum* 8 (2024). doi:10.22331/q-2024-01-11-1226
- Christoph Sünderhauf, Zalán Németh, Adnaan Walayat, Andrew Patterson, and Bjorn K. Berntson. 2025. Matrix inversion polynomials for the quantum singular value transformation. arXiv:2507.15537 [quant-ph] doi:10.48550/arXiv.2507.15537

- Ewin Tang. 2019. A quantum-inspired classical algorithm for recommendation systems. In *ACM Symposium on Theory of Computing*. doi:10.1145/3313276.3316310
- Ross Tate, Michael Stepp, Zachary Tatlock, and Sorin Lerner. 2011. Equality Saturation: A New Approach to Optimization. *Logical Methods in Computer Science* 7, 1 (2011). doi:10.2168/LMCS-7(1:10)2011
- Stanimire Tomov, Jack Dongarra, and Marc Baboulin. 2010. Towards dense linear algebra for hybrid GPU accelerated manycore systems. *Parallel Comput.* 36, 5-6 (2010). doi:10.1016/j.parco.2009.12.005
- Nathaniel Tornow, Emmanouil Giortamis, and Pramod Bhatotia. 2025. QVM: Quantum Gate Virtualization Machine. In *ACM SIGPLAN Conference on Programming Language Design and Implementation*. doi:10.1145/3729290
- Wim van Dam, Mariia Mykhailova, and Mathias Soeken. 2023. Using Azure Quantum Resource Estimator for Assessing Performance of Fault Tolerant Quantum Computation. In *Workshops of the International Conference on High Performance Computing, Network, Storage, and Analysis*. doi:10.1145/3624062.3624211
- Field G. Van Zee, Ernie Chan, Robert A. van de Geijn, Enrique S. Quintana-Ortí, and Gregorio Quintana-Ortí. 2009. The libflame Library for Dense Matrix Computations. *Computing in Science & Engineering* 11, 6 (2009). doi:10.1109/MCSE.2009.207
- Matan Vax, Peleg Emanuel, Eyal Cornfeld, Israel Reichental, Ori Opher, Ori Roth, Tal Michaeli, Lior Preminger, Lior Gazit, Amir Naveh, and Yehuda Naveh. 2025. Qmod: Expressive High-Level Quantum Modeling. arXiv:2502.19368 [quant-ph] doi:10.48550/arXiv.2502.19368
- Finn Voichick, Liyi Li, Robert Rand, and Michael Hicks. 2023. Qunity: A Unified Language for Quantum and Classical Computing. In *ACM SIGPLAN Symposium on Principles of Programming Languages*. doi:10.1145/3571225
- R. Clint Whaley and Jack Dongarra. 1998. Automatically tuned linear algebra software. In *ACM/IEEE Conference on Supercomputing*. doi:10.1109/SC.1998.10004
- Amanda Xu, Abtin Molavi, Lauren Pick, Swamit Tannu, and Aws Albarghouthi. 2023. Synthesizing Quantum-Circuit Optimizers. In *ACM SIGPLAN Conference on Programming Language Design and Implementation*. doi:10.1145/3591254
- Amanda Xu, Abtin Molavi, Swamit Tannu, and Aws Albarghouthi. 2025b. Optimizing Quantum Circuits, Fast and Slow. In *ACM International Conference on Architectural Support for Programming Languages and Operating Systems*. doi:10.1145/3669940.3707240
- Mingkuan Xu, Zikun Li, Oded Padon, Sina Lin, Jessica Pointing, Auguste Hirth, Henry Ma, Jens Palsberg, Alex Aiken, Umut A. Acar, and Zhihao Jia. 2022. Quartz: Superoptimization of Quantum Circuits. In *ACM SIGPLAN Conference on Programming Language Design and Implementation*. doi:10.1145/3519939.3523433
- Yingte Xu, Gilles Barthe, and Li Zhou. 2025a. Automating Equational Proofs in Dirac Notation. In *ACM SIGPLAN Symposium on Principles of Programming Languages*. doi:10.1145/3704878
- Chao-Hua Yu, Fei Gao, and Qiao-Yan Wen. 2021. An Improved Quantum Algorithm for Ridge Regression. *IEEE Transactions on Knowledge & Data Engineering* 33, 03 (2021). doi:10.1109/TKDE.2019.2937491
- Charles Yuan. 2026. *Cobble: Compiling Block Encodings for Quantum Computational Linear Algebra*. doi:10.5281/zenodo.18898778
- Charles Yuan and Michael Carbin. 2022. Tower: Data Structures in Quantum Superposition. In *ACM SIGPLAN Conference on Object-Oriented Programming, Systems, Languages, and Applications*. doi:10.1145/3563297
- Charles Yuan, Agnes Villanyi, and Michael Carbin. 2024. Quantum Control Machine: The Limits of Control Flow in Quantum Programming. In *ACM SIGPLAN Conference on Object-Oriented Programming, Systems, Languages, and Applications*. doi:10.1145/3649811
- Zhicheng Zhang and Mingsheng Ying. 2025. Quantum Register Machine: Efficient Implementation of Quantum Recursive Programs. In *ACM SIGPLAN Conference on Programming Language Design and Implementation*. doi:10.1145/3729283

Received 2025-11-04; accepted 2026-04-03